Thermodynamic speed limits in isolated quantum systems

Rikuya Kobashi *
Department of Physics, Kyoto University, Kyoto 606-8502, Japan

(Received 18 February 2026; accepted 6 October 2026; published 9 November 2026)

We derive thermodynamic speed limits for isolated quantum systems undergoing finite-time unitary driving. The key ingredient is a set of generalized second-law inequalities: For the Gibbs entropy and for several thermodynamically motivated observational entropies, the entropy production is bounded from below by a function of the Vu-Saito quantum Wasserstein distance between the initial and final coarse-grained states. These inequalities yield lower bounds on the operation time in terms of the average entropy-production rate. We apply the framework to system-bath coarse graining, local-energy coarse graining, and diagonal entropy, and illustrate the resulting bounds with numerical and analytically solvable examples. Our results provide a thermodynamic characterization of finite-time state transformations in isolated quantum systems and clarify how coarse-grained entropy production constrains macroscopic reachability.

DOI: 10.1103/k16k-nx74

I. INTRODUCTION

Is it possible, in principle, to move through space or to make computers perform calculations at arbitrarily high speed? Prior studies indicate that fundamental physical laws constrain not only energetic and entropic resources but also the rate at which physical states—and hence information processing—can be transformed. In isolated quantum systems, this constraint is formalized as the quantum speed limit: The minimum time required to implement a given evolution is bounded from below by the energy fluctuations [1] or the mean energy [2], together with a geometric distance between the initial and final states [3,4]. Such speed-limit inequalities are important not only from a fundamental perspective but also for a wide range of tasks based on isolated quantum systems—such as state transfer, optimal control, and related tasks—where they set intrinsic bounds on performance [5–8].

Speed limits are not unique to isolated quantum systems. For open systems, whose dynamics is constrained by thermodynamics, it is natural to ask how speed limits are related to thermodynamic quantities. In the field of stochastic thermodynamics, the rate of change of the state distribution is constrained by trade-offs involving entropy production and dynamical activity [9–13]. These bounds are now regarded as fundamental constraints in nonequilibrium thermodynamics. Similar speed-limit relations have also been reported for Lindblad-type open quantum systems [14].

Recent progress in stochastic thermodynamics has been further propelled by incorporating optimal transport theory [15]. Optimal transport theory is a mathematical framework that has been developed to construct optimal protocols for transforming one probability distribution into another [16]. Many tasks realized using physical systems can be viewed precisely as processes that transform an initial distribution into a desired target distribution. It is therefore not surprising that insights from physics concerning such tasks are closely related to optimal transport theory. In particular, it is known that, in stochastic thermodynamic systems, the minimum entropy production required to perform a given task is intimately connected to the L_2-Wasserstein distance familiar in the overdamped Langevin dynamics [17]. Moreover, this interplay between thermodynamics and optimal transport has also been developed for the Markov jump process as well as Lindblad-type open quantum systems [18]. By defining a quantum Wasserstein distance as a quantum extension of the classical Wasserstein metric, previous work derived a Benamou-Brenier-type identity and established new speed-limit bounds.

Understanding how phenomena that appear irreversible on macroscopic scales can be reconciled with the reversible dynamics of isolated quantum systems has long been a fundamental problem. With recent advances in quantum simulators such as ultracold atoms and trapped-ion platforms, the problem of thermalization and equilibration in isolated quantum systems has seen rapid progress on both theoretical and experimental fronts [19–24]. In parallel, substantial effort has been devoted to examining whether an isolated quantum system, once equilibrated, is consistent with macroscopic thermodynamic laws. In particular, a long-running line of work has focused on microscopic formulations of thermodynamic quantities. Within this approach, thermodynamic behavior, including the second law, is derived directly from the unitary dynamics of isolated quantum systems in a variety of settings [25–28]. A basic obstacle is that under strictly unitary time evolution the von Neumann entropy is conserved, and thus cannot by itself capture irreversibility. To address this, alternative entropy notions have been proposed, notably, observational entropy [29–32]—including the diagonal entropy

*Contact author: kobashi.rikuya.84s@st.kyoto-u.ac.jp

Published by the American Physical Society under the terms of the Creative Commons Attribution 4.0 International license. Further distribution of this work must maintain attribution to the author(s) and the published article's title, journal citation, and DOI.

[33,34]—and the Gibbs entropy [35,36]. These entropies satisfy thermodynamic differential relations when the system is in equilibrium and can increase under driving, thereby providing entropy measures that are compatible with the second law for isolated quantum dynamics.

As reviewed above, thermal behavior can emerge even in isolated systems. However, in contrast to open-system, finite-time thermodynamic constraints for isolated dynamics—e.g., thermodynamic speed limits—still appear to be far from fully understood. At the same time, to the best of our knowledge, the connection between nonequilibrium phenomena in isolated systems and optimal transport theory remains largely unexplored. In light of these considerations, we build on the recent understanding of thermalization in isolated quantum systems and on microscopic derivations of the second law. We then develop a more quantitative characterization of entropy production, based on thermodynamically meaningful entropies and quantified using a quantum Wasserstein distance.

The main contributions of this work are threefold. First, we derive generalized second-law inequalities for isolated quantum systems, in which entropy production associated with the Gibbs entropy and observational entropy is bounded from below by the Vu-Saito quantum Wasserstein distance. Second, we apply these inequalities to thermodynamically motivated coarse grainings, including system-bath, local-energy, and energy-basis coarse grainings. Third, by dividing the entropy-production bounds by the average entropy-production rate, we obtain thermodynamic speed limits for finite-time unitary protocols.

The remainder of this paper is organized as follows. In Sec. II, we introduce the setup. In Sec. III, we define the Gibbs entropy, observational entropy, and the Vu-Saito quantum Wasserstein distance. In Sec. IV, we present the generalized second laws and derive the corresponding speed limits. In Sec. V, we discuss applications and numerical demonstrations. In Sec. VI, we provide the derivations of the main results. Section VII is devoted to conclusions and outlook.

II. SETUP

We consider an isolated quantum system on a d-dimensional Hilbert space $\mathcal{H}$. Its state is represented by a density operator ρ, satisfying $\rho \geqslant 0$ and $\mathrm{tr}[\rho] = 1$. The dynamics are generated by a generally time-dependent Hamiltonian $H(\lambda_t)$, where λ_t denotes an external control parameter. We write the spectral decomposition as

$$H(\lambda) = \sum_{i=1}^{n} E_i(\lambda)\hat{P}_i^{(E)}(\lambda), \tag{1}$$

where $E_i(\lambda)$ is the ith energy eigenvalue in increasing order and $\hat{P}_i^{(E)}(\lambda)$ is the corresponding spectral projector.

We use projective measurements as coarse grainings of the Hilbert space. A projection-valued measure (PVM) $\mathcal{C} = \{\hat{P}_x\}_{x\in\mathcal{X}}$ satisfies $\sum_x \hat{P}_x = \hat{I}$ and $\hat{P}_x\hat{P}_{x'} = \delta_{xx'}\hat{P}_x$. For a state ρ, the probability of outcome x is $p_x = \mathrm{tr}[\hat{P}_x\rho]$. We call ρ a macroscopic state with respect to $\mathcal{C}$ if

$$\rho = \sum_x p_x \frac{\hat{P}_x}{V_x}, \quad V_x = \mathrm{tr}[\hat{P}_x]. \tag{2}$$

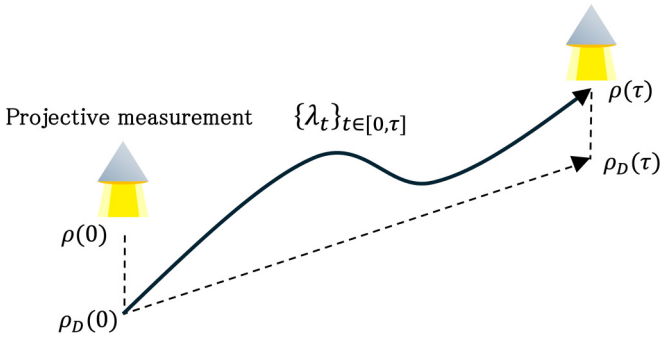


FIG. 1. Schematic of the two-point coarse-graining protocol for an isolated quantum system.

For an arbitrary state ρ, the associated coarse-grained state is

$$\rho_{\mathcal{C}} := \sum_x \mathrm{tr}[\hat{P}_x\rho]\frac{\hat{P}_x}{V_x}. \tag{3}$$

One Kraus representation of this map is obtained by choosing an orthonormal basis $\{|x,a\rangle\}_{a=1}^{V_x}$ of the image of $\hat{P}_x$ and setting

$$K_{x,a,b} = \frac{1}{\sqrt{V_x}}|x,a\rangle\langle x,b|, \quad a,b = 1,\ldots,V_x. \tag{4}$$

This representation is used only to make explicit that $\rho_{\mathcal{C}}$ can be realized as an unselective measurement outcome.

We now specify the protocol used throughout the paper. The system is initially prepared with control parameter λ_0 and state $\rho(0)$. Immediately before the unitary evolution, we apply the coarse-graining measurement associated with the initial PVM $\mathcal{C}_i = \{\hat{P}_x\}_x$, so that the initial state becomes $\rho_{\mathcal{C}_i}(0)$. The system then evolves unitarily during $0 \leqslant t \leqslant \tau$ under the externally controlled Hamiltonian $H(\lambda_t)$. At the end of the protocol, the final PVM $\mathcal{C}_f = \{\hat{Q}_y\}_y$ is applied, yielding

$$\rho_{\mathcal{C}_f}(\tau) = \sum_y q_y \frac{\hat{Q}_y}{\mathrm{tr}[\hat{Q}_y]}, \quad q_y = \mathrm{tr}[\hat{Q}_y\rho(\tau)]. \tag{5}$$

This two-point coarse-graining framework allows us to compare entropy-related quantities at the beginning and at the end of the unitary protocol (see Fig. 1).

III. THERMODYNAMIC ENTROPIES AND QUANTUM TRANSPORT DISTANCE

A. Entropy production in isolated quantum systems

Understanding thermodynamic irreversibility from the reversible dynamics of isolated systems is a central problem in statistical mechanics. The microscopic time evolution of an isolated quantum system is unitary and therefore preserves the fine-grained von Neumann entropy,

$$S_{\mathrm{vN}}(\rho(t)) = -\mathrm{tr}[\rho(t)\ln\rho(t)] = S_{\mathrm{vN}}(\rho(0)). \tag{6}$$

This conservation seems, at first sight, to be in tension with the thermodynamic description of many-body systems, where relaxation, thermalization, and entropy increase are observed as irreversible phenomena.

One resolution is that thermodynamic irreversibility is not a property of the full microscopic state alone, but of a coarse-grained description of that state. Thermodynamics does not

track all microscopic degrees of freedom. Instead, it describes a many-body system in terms of macroscopic variables such as energy, particle number, external control parameters, and local conserved quantities. Many distinct microscopic states are therefore identified as the same thermodynamic macrostate. From this viewpoint, irreversibility appears when microscopic information becomes irrelevant or inaccessible within the chosen coarse-grained description, even though the underlying unitary dynamics remains reversible.

For this reason, entropy production in isolated quantum systems should be defined at the same level of description as the relevant macroscopic variables. In what follows, we introduce two such entropy functionals: the Gibbs entropy and observational entropy. A PVM will be used as the mathematical representation of a coarse graining because it partitions the Hilbert space into mutually orthogonal macrospaces and identifies microscopic states that yield the same macroscopic observable values as the same coarse-grained macrostate.

B. Gibbs entropy

The Gibbs entropy is one of the most fundamental entropies that describes thermodynamic properties in equilibrium and satisfies an entropy-increase law under thermodynamic operations. In equilibrium at energy E and control parameter λ, the Gibbs entropy is defined by

$$S_G(E,\lambda) := k_B \ln \mathrm{tr}\Theta(E - H(\lambda)), \tag{7}$$

where

$$\Theta(E - H(\lambda)) := \sum_{i:\, E_i(\lambda)\leqslant E} \hat{P}_i^{(E)}(\lambda) \tag{8}$$

denotes the spectral projection of $H(\lambda)$ onto the subspace of the Hilbert space spanned by eigenstates with eigenvalues not exceeding E. In the following, we set $k_B := 1$. In thermodynamically large systems, the Gibbs entropy is known to asymptotically coincide with the Boltzmann entropy.

To examine the validity of the present entropy, we first focus on the fundamental thermodynamic relations that thermodynamic entropy must satisfy. In thermodynamics, the entropy is defined as a function of the energy and the volume, and it is required to satisfy

$$\frac{\partial S}{\partial E} = \frac{1}{T}, \quad \frac{\partial S}{\partial V} = \frac{p}{T}, \tag{9}$$

where V, p, and T denote the system volume, the thermodynamic pressure, and the absolute temperature, respectively. We next show that an analogous structure also holds for the Gibbs entropy S_G adopted in this work. Introducing the "Gibbs temperature" T_G and the microscopic pressure p_λ^{mic} through

$$\frac{1}{T_G} := \frac{\partial S_G}{\partial E}, \quad p_\lambda^{\mathrm{mic}} := -\mathrm{tr}\left[\frac{\partial H(\lambda)}{\partial \lambda}\rho^{\mathrm{mic}}(E,\lambda)\right], \tag{10}$$

we find that

$$\frac{\partial S_G}{\partial \lambda} = \frac{p_\lambda^{\mathrm{mic}}}{T_G} \tag{11}$$

holds. Here, the microcanonical state $\rho^{\mathrm{mic}}(E,\lambda)$ and the density of states $W(E,\lambda)$ are defined as

$$\rho^{\mathrm{mic}}(E,\lambda) := \sum_{i=1}^{d} \frac{\delta(E_i(\lambda) - E)}{W(E,\lambda)} |i_\lambda\rangle\langle i_\lambda|, \tag{12}$$

$$W(E,\lambda) := \sum_{i=1}^{d} \delta(E_i(\lambda) - E), \tag{13}$$

respectively. Thus, S_G satisfies differential relations analogous to those of the conventional thermodynamic entropy, making it a natural definition in this sense. However, it should be noted that the above reasoning implicitly assumes the validity of $T_G(E)$ itself. When examining this validity, one must consider issues such as the possibility of negative temperature and the requirement that two systems in thermal contact at equilibrium share the same temperature. These matters are closely related to—and often discussed together with—the consistency between the Gibbs entropy and the Boltzmann entropy, which represent distinct microscopic formulations of thermodynamic entropy (see, e.g., Refs. [37–40]).

We emphasize that the Gibbs entropy possesses an important property relevant for its extension to nonequilibrium states—namely, the thermodynamic second law—as will be discussed below. In this paper, we consider

$$S_G(\rho, H(\lambda)) := \sum_{i=1}^{n}\sum_{k=1}^{d_i} \ln(n_{i-1}+k) \frac{\mathrm{tr}\left[\hat{P}_i^{(E)}(\lambda)\rho\right]}{\mathrm{tr}\left[\hat{P}_i^{(E)}(\lambda)\right]}, \tag{14}$$

$$n_i = n_{i-1} + d_i, \quad d_i = \mathrm{tr}\left[\hat{P}_i^{(E)}(\lambda)\right], \quad n_0 = 0 \tag{15}$$

an extension of this definition that remains well defined for nonequilibrium states as well. By choosing ρ as the microcanonical state $\rho^{\mathrm{mic}}(E,\lambda)$, the definition becomes consistent with that of the equilibrium state.

When the initial state ρ is passive, namely, when ρ is diagonal in the eigenbasis $\{|i(\lambda_0)\rangle\}_{i=1}^n$ of the Hamiltonian $H(\lambda_0)$ and satisfies for

$$\frac{\mathrm{tr}\left[\hat{P}_i^{(E)}(\lambda)[\rho]\right]}{\mathrm{tr}\left[\hat{P}_i^{(E)}(\lambda)\right]} \leqslant \frac{\mathrm{tr}\left[\hat{P}_j^{(E)}(\lambda)[\rho]\right]}{\mathrm{tr}\left[\hat{P}_j^{(E)}(\lambda)\right]} \tag{16}$$

$\forall i > j$, the second-law-like relation

$$S_G(U\rho U^\dagger, H(\lambda_\tau)) \geqslant S_G(\rho, H(\lambda_0)) \tag{17}$$

holds [36]. Note that $E_i(\lambda)$ is the ith energy eigenvalue in increasing order. For any passive state, the unitary operator that achieves the equality is, up to irrelevant phase degrees of freedom, uniquely given by $U_{\mathrm{ad}} := \sum_{n=1}^{d} |n_{\lambda_\tau}\rangle\langle n_{\lambda_0}|$ (see Appendix B).

C. Observational entropy and thermodynamic coarse grainings

Although the Gibbs entropy is a fundamental thermodynamic entropy for isolated systems, it is tied to the energy ordering and therefore cannot capture all forms of macroscopic relaxation. For example, relaxation under a fixed Hamiltonian can be visible at the level of local observables even when the Gibbs entropy does not change. To describe entropy production associated with more general thermodynamic macrostates, we use observational entropy.

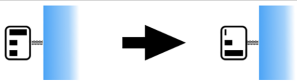
Coarse-grainings	Physical Situations	Typical initial macrostate
$\mathcal{C}_{\rho,H_B} \equiv \{\hat{P}_i^{(\rho)} \otimes \Pi_j^B\}_{ij}$ System-Bath Coarse-graining	 Small system coupled to a large bath	$\rho_s \otimes \pi_B$ π_B : Bath's equilibrium
$\mathcal{C}_{\mathrm{loc}H} \equiv \left\{\hat{P}_{\vec{E}}\right\}_{\vec{E}}$ Factorized observational entropy	 Global relaxation & Hydrodynamic-type relaxation	$\bigotimes_\ell \rho_\ell \quad [\rho_\ell, H_\ell] = 0$ Local equilibrium
$\mathcal{C}_{H(\lambda)} \equiv \left\{\hat{P}_i(\lambda)\right\}_i$ Diagonal entropy	 Driven isolated systems and quantum quenches	Energy-diagonal state

FIG. 2. Thermodynamic coarse grainings used for observational entropy. The system-bath coarse graining resolves the bath-energy shell and the eigenbasis of the reduced-system state; the local-energy coarse graining resolves the energy profile over spatial cells; and the energy coarse graining gives the diagonal entropy.

General definition. Let $\mathcal{C} = \{\hat{P}_x\}_x$ be a coarse graining of the Hilbert space. For a state ρ, define

$$p_x = \mathrm{tr}[\hat{P}_x \rho], \quad V_x = \mathrm{tr}[\hat{P}_x]. \tag{18}$$

The observational entropy associated with $\mathcal{C}$ is

$$S_{\mathrm{obs}}^{\mathcal{C}}(\rho) := -\sum_x p_x \ln \frac{p_x}{V_x}. \tag{19}$$

Equivalently,

$$S_{\mathrm{obs}}^{\mathcal{C}}(\rho) = -\sum_x p_x \ln p_x + \sum_x p_x \ln V_x. \tag{20}$$

The first term is the Shannon entropy of the coarse-grained outcome distribution, while the second term is the average logarithmic volume of the corresponding macrospaces. Since coarse graining discards microscopic information,

$$S_{\mathrm{obs}}^{\mathcal{C}}(\rho) \geqslant S_{\mathrm{vN}}(\rho). \tag{21}$$

If the initial state is already macroscopic with respect to $\mathcal{C}$, this inequality and the conservation of S_{vN} imply

$$S_{\mathrm{obs}}^{\mathcal{C}}(\rho_t) \geqslant S_{\mathrm{obs}}^{\mathcal{C}}(\rho_0). \tag{22}$$

Thus, the increase of observational entropy reflects the loss of information induced by the macroscopic description, not microscopic irreversibility.

Observational entropy depends on the chosen coarse graining. Hence, only coarse grainings associated with thermodynamic observables should be interpreted as thermodynamic entropies. In this work, we use the three coarse grainings summarized in Fig. 2.

Thermodynamic coarse grainings. We consider three thermodynamically motivated coarse grainings.

Thermodynamic speed limits derived for Lindblad dynamics should admit a unitary system-bath description such as in Ref. [41]. We therefore first consider an isolated system decomposed into a small system and a bath. For a small system S coupled to a bath B, let

$$\Pi_j^B := \mathbf{1}_j(H_B), \quad \rho_S := \mathrm{tr}_B[\rho] = \sum_i \nu_i \hat{P}_i^{(\rho_S)}, \tag{23}$$

where Π_j^B projects onto the jth mesoscopic bath-energy window. We define the system-bath coarse graining by

$$\mathcal{C}_{\rho,H_B} := \left\{\hat{P}_i^{(\rho_S)} \otimes \Pi_j^B\right\}_{ij}. \tag{24}$$

This coarse graining resolves the reduced-system eigenspaces and the bath-energy windows. Its relation to the conventional open-system entropy production is discussed in Appendix A 1.

For an isolated many-body system with

$$H = \sum_{\ell=1}^m H_\ell + H_{\mathrm{int}}, \quad H_\ell = \sum_{E_\ell} E_\ell \hat{P}_{E_\ell}^{(\ell)}, \tag{25}$$

we define the local-energy coarse graining and the corresponding factorized observational entropy (FOE) by

$$\mathcal{C}_{\mathrm{loc}H} := \left\{\bigotimes_{\ell=1}^m \hat{P}_{E_\ell}^{(\ell)}\right\}_{\vec{E}}, \quad S_{\mathrm{FOE}}(\rho) := S_{\mathrm{obs}}^{\mathcal{C}_{\mathrm{loc}H}}(\rho). \tag{26}$$

This coarse graining resolves the spatial energy profile and is appropriate for local and hydrodynamic relaxation.

Finally, for the spectral projectors $\hat{P}_i^{(E)}(\lambda)$ of $H(\lambda)$, we define

$$\mathcal{C}_{H(\lambda)} := \left\{\hat{P}_i^{(E)}(\lambda)\right\}_i, \quad S_D(\rho; H(\lambda)) := S_{\mathrm{obs}}^{\mathcal{C}_{H(\lambda)}}(\rho). \tag{27}$$

This coarse graining resolves the global energy occupations and is appropriate for driven isolated systems and quantum quenches. For a nondegenerate Hamiltonian, S_D reduces to the conventional diagonal entropy.

The corresponding physical settings and typical initial macrostates are summarized in Fig. 2. Detailed definitions and physical interpretations of these three thermodynamic coarse grainings are provided in Appendix A.

D. Quantum Wasserstein distance

In this paper, we employ the Vu-Saito quantum Wasserstein distance (VS-QW) introduced by Ref. [18], defined as

$$\mathcal{W}_q(\rho, \sigma) := \tfrac{1}{2} \min_{V^\dagger V = \mathbb{I}} \|V\rho V^\dagger - \sigma\|_1. \tag{28}$$

Here, $\|\rho-\sigma\|_1 := \mathrm{tr}\sqrt{(\rho-\sigma)^\dagger(\rho-\sigma)}$. The minimum is taken over all unitary transformations V. VS-QW was introduced to extend an important property, which holds for classical fluctuating systems, to open quantum systems described by the Lindblad equation [42,43]. In our results, two features of VS-QW play a central role: It admits a closed-form expression in terms of the eigenvalues of a given quantum state, and it is a pseudometric [i.e., $\mathcal{W}_q(\rho,\sigma)=0$ is possible for $\rho\neq\sigma$]. Since $\mathcal{W}_q$ depends only on the spectra of the two states, $\mathcal{W}_q(\rho,\sigma)=0$ means unitary equivalence rather than equality of density matrices. Specifically, the closed-form expression reads

$$\mathcal{W}_q(\rho,\sigma)=\frac{1}{2}\sum_{i=1}^{d}|\mu_i(\rho)-\mu_i(\sigma)|, \tag{29}$$

where $\{\mu_i(\rho)\}_{i=1}^d$ and $\{\mu_i(\sigma)\}_{i=1}^d$ are increasing eigenvalues of ρ and σ, respectively.

IV. MAIN RESULTS

We now present the generalized second-law inequalities and the resulting thermodynamic speed limits. The main message is that, for suitable coarse-grained entropies, entropy production lower bounds the Vu-Saito quantum Wasserstein distance between the initial and final coarse-grained states. Dividing this entropy-production bound by the average entropy-production rate gives a lower bound on the operation time.

A. Gibbs-entropy bound

Theorem 1: *Gibbs entropy*. Assume that the initial state $\rho(0)$ is passive with respect to the initial Hamiltonian $H(\lambda_0)$. Define the Gibbs entropy production by

$$\Delta S_G(\tau) := S_G(\rho(\tau),H(\lambda_\tau))-S_G(\rho(0),H(\lambda_0)), \tag{30}$$

and define

$$\mathcal{W}_q^G := \mathcal{W}_q(\rho_{\mathcal{C}_{H(\lambda_\tau)}}(\tau),\rho(0)). \tag{31}$$

Then,

$$\Delta S_G(\tau)\geqslant \ln 2\left(\mathcal{W}_q^G\right)^2. \tag{32}$$

Consequently, with

$$\langle\sigma_G\rangle_\tau := \frac{\Delta S_G(\tau)}{\tau}, \tag{33}$$

we obtain the speed limit

$$\tau\geqslant \ln 2\,\frac{\left(\mathcal{W}_q^G\right)^2}{\langle\sigma_G\rangle_\tau} =: \tau_{G,2}. \tag{34}$$

This bound states that, at a fixed average Gibbs entropy-production rate, a finite redistribution of the energy occupation distribution requires a finite operation time. It is relevant to finite-time driving, quantum quenches, and shortcuts to adiabaticity (STA) in isolated quantum systems.

For finite-dimensional systems, a sharper linear bound is also available:

$$\Delta S_G(\tau)\geqslant \ln\left(\frac{d}{d-1}\right)\mathcal{W}_q^G, \tag{35}$$

$$\tau\geqslant \ln\left(\frac{d}{d-1}\right)\frac{\mathcal{W}_q^G}{\langle\sigma_G\rangle_\tau} =: \tau_{G,1}. \tag{36}$$

Here, d is the Hilbert-space dimension. In particular, for a two-level system this linear bound is always tighter than Eq. (32). The proofs of Eqs. (32) and (35) are given in Sec. VI.

B. Bounds for observational entropy production

1. General bound

Theorem 2: *Observational entropy*. Let $\mathcal{C}^i=\{\hat{P}_x\}_x$ and $\mathcal{C}^f=\{\hat{Q}_y\}_y$ be the initial and final coarse grainings. Assume that the initial state is macroscopic with respect to $\mathcal{C}^i$,

$$\rho(0)=\rho_{\mathcal{C}^i}(0) := \sum_x p_x(0)\frac{\hat{P}_x}{V_x}. \tag{37}$$

After the unitary evolution $\rho(\tau)=U(\tau)\rho(0)U^\dagger(\tau)$, the final coarse-grained state is

$$\rho_{\mathcal{C}^f}(\tau) := \sum_y q_y(\tau)\frac{\hat{Q}_y}{V_y}. \tag{38}$$

The observational entropy production is

$$\Delta S_{\mathcal{C}^i\to\mathcal{C}^f}(\tau) := S_{\mathrm{obs}}^{\mathcal{C}^f}(\rho(\tau))-S_{\mathrm{obs}}^{\mathcal{C}^i}(\rho(0)). \tag{39}$$

Then,

$$\Delta S_{\mathcal{C}^i\to\mathcal{C}^f}(\tau)\geqslant 2\mathcal{W}_q(\rho_{\mathcal{C}^f}(\tau),\rho(0))^2. \tag{40}$$

This inequality gives a quantitative form of the entropy-increase law. A final coarse-grained state that is separated from the initial macrostate by a finite VS-QW distance necessarily requires a finite amount of observational entropy production.

Defining the average observational entropy-production rate by

$$\bar{\sigma}_{\mathcal{C}^i\to\mathcal{C}^f}(\tau) := \frac{\Delta S_{\mathcal{C}^i\to\mathcal{C}^f}(\tau)}{\tau}, \tag{41}$$

we obtain the corresponding speed limit

$$\tau\geqslant \frac{2\mathcal{W}_q(\rho_{\mathcal{C}^f}(\tau),\rho(0))^2}{\bar{\sigma}_{\mathcal{C}^i\to\mathcal{C}^f}(\tau)}. \tag{42}$$

Thus, if the average entropy-production rate is fixed, a process that changes the macrostate by a finite distance cannot be completed in an arbitrarily short time.

The inequality also gives a compact reachability interpretation. For the operation in which a state is first coarse grained with respect to $\mathcal{C}$ and then transformed unitarily, observational entropy is a monotone. Equation (40) strengthens this monotonicity quantitatively: Whenever the reverse transformation is impossible because the final and initial coarse-grained spectra are separated, the entropy ordering becomes strict. In this sense, Eqs. (32) and (40) are generalized second-law inequalities.

The same mathematical result can also be applied to nonthermodynamic coarse grainings. As an example, Appendix D discusses the entanglement entropy of bipartite pure states.

2. Thermodynamic specializations

$\mathcal{C}_{\rho,H_B}$coarse graining. We first apply the general inequality to the system-bath coarse graining $\mathcal{C}_{\rho,H_B}$. As the initial state,

we assume

$$\rho(0) = \rho_s(0) \otimes \pi_B, \quad \pi_B = \frac{e^{-\beta \tilde{H}_B}}{\tilde{Z}_B}. \tag{43}$$

We define the corresponding observational entropy production, the conventional open-system entropy production, and the Vu-Saito quantum Wasserstein distance by

$$\Delta S_{\mathrm{SB}}(\tau) := S_{\mathrm{obs}}^{\mathcal{C}_{\rho(\tau),H_B}}(\rho(\tau)) - S_{\mathrm{obs}}^{\mathcal{C}_{\rho(0),H_B}}(\rho(0)), \tag{44}$$

$$\Sigma_\tau := D(\rho(\tau) \,\|\, \rho_S(\tau) \otimes \pi_B), \tag{45}$$

$$\mathcal{W}_q^{\mathrm{open}} := \mathcal{W}_q\big(\rho_{\mathcal{C}_{\rho(\tau),H_B}}(\tau), \rho_S(0) \otimes \pi_B\big), \tag{46}$$

where $\rho_S(\tau) = \mathrm{tr}_B[\rho(\tau)]$. Here, $D(\cdot\|\cdot)$ denotes the Umegaki relative entropy. Under the assumptions above, Σ_τ is equivalently expressed as

$$\Sigma_\tau = \Delta S_{\mathrm{vN}}(\rho_S) + \beta Q_\tau. \tag{47}$$

The detailed definitions of the system-bath coarse graining, the bath heat Q_τ, and the derivation of this equivalence are given in Appendix A 1.

Then, we obtain

$$\Sigma_\tau \geqslant \Delta S_{\mathcal{C}_{\rho(0),H_B} \to \mathcal{C}_{\rho(\tau),H_B}}(\tau) \geqslant 2\big(\mathcal{W}_q^{\mathrm{open}}\big)^2. \tag{48}$$

Equivalently, by introducing the average entropy-production rates

$$\bar{\sigma}_{\mathcal{C}_{\rho(0),H_B} \to \mathcal{C}_{\rho(\tau),H_B}}(\tau) := \frac{\Delta S_{\mathcal{C}_{\rho(0),H_B} \to \mathcal{C}_{\rho(\tau),H_B}}(\tau)}{\tau}, \tag{49}$$

$$\sigma_\tau := \frac{\Sigma_\tau}{\tau}, \tag{50}$$

we obtain the thermodynamic speed-limit inequality

$$\tau \geqslant \frac{2\big(\mathcal{W}_q^{\mathrm{open}}\big)^2}{\bar{\sigma}_{\mathcal{C}_{\rho(0),H_B} \to \mathcal{C}_{\rho(\tau),H_B}}(\tau)} \tag{51}$$

$$\geqslant \frac{2\big(\mathcal{W}_q^{\mathrm{open}}\big)^2}{\sigma_\tau}. \tag{52}$$

These inequalities apply to a small system interacting with a large bath. They provide an isolated-system route to open-system thermodynamic speed limits, with the important distinction that the VS-QW is evaluated for the coarse-grained state of the total system, including the bath.

Factorized observational entropy. Next, we consider the factorized observational entropy associated with the local-energy coarse graining $\mathcal{C}_{\mathrm{loc}H}$. We assume that the initial state is given by a product of states that are diagonal with respect to the corresponding local Hamiltonians:

$$\rho(0) = \bigotimes_\ell \rho_\ell(0), \quad [\rho_\ell(0), H_\ell] = 0. \tag{53}$$

We denote the corresponding factorized observational entropy production and the Vu-Saito quantum Wasserstein distance by

$$\Delta S_{\mathrm{FOE}}(\tau) := S_{\mathrm{FOE}}(\rho(\tau)) - S_{\mathrm{FOE}}(\rho(0)), \tag{54}$$

$$\mathcal{W}_q^{\mathrm{FOE}} := \mathcal{W}_q(\rho_{\mathcal{C}_{\mathrm{loc}H}}(\tau), \rho(0)). \tag{55}$$

Substituting $\mathcal{C}^i = \mathcal{C}^f = \mathcal{C}_{\mathrm{loc}H}$ into the general inequality, we obtain

$$\Delta S_{\mathrm{FOE}}(\tau) \geqslant 2\big(\mathcal{W}_q^{\mathrm{FOE}}\big)^2. \tag{56}$$

Equivalently, by introducing the average production rate

$$\bar{\sigma}_{\mathrm{FOE}}(\tau) := \frac{\Delta S_{\mathrm{FOE}}(\tau)}{\tau}, \tag{57}$$

we obtain the thermodynamic speed-limit inequality

$$\tau \geqslant \frac{2\big(\mathcal{W}_q^{\mathrm{FOE}}\big)^2}{\bar{\sigma}_{\mathrm{FOE}}(\tau)}. \tag{58}$$

This inequality bounds how fast an isolated many-body system can change its local-energy profile at a fixed rate of factorized observational entropy production. It can therefore be regarded as a finite-size precursor of a hydrodynamic relaxation bound.

If the relaxation time of a hydrodynamic mode is defined as the time required for the initial coarse-grained local-energy distribution to reach the state in which the mode becomes spatially uniform, the FOE speed limit directly gives a lower bound on this relaxation time. Let the initial FOE macrostate and the uniform FOE macrostate be denoted by

$$\rho_{\mathrm{FOE}}^{\mathrm{ini}}, \quad \rho_{\mathrm{FOE}}^{\mathrm{unif}}. \tag{59}$$

Then, the relaxation time satisfies

$$\tau_{\mathrm{rel}} \geqslant \frac{2\big(\mathcal{W}_q^{\mathrm{FOE}}\big)^2}{\bar{\sigma}_{\mathrm{FOE}}(\tau_{\mathrm{rel}})}. \tag{60}$$

This inequality shows that a hydrodynamic mode whose initial profile is separated from the uniform profile by a finite FOE Wasserstein distance cannot relax in an arbitrarily short time, unless the average FOE entropy-production rate becomes correspondingly large.

Diagonal entropy. Finally, we consider the diagonal entropy associated with the energy coarse-graining $\mathcal{C}_{H(\lambda)}$. In this specialization, we assume that the initial state is diagonal in the energy eigenbasis of the initial Hamiltonian. We abbreviate the corresponding diagonal entropy production and the Vu-Saito quantum Wasserstein distance as

$$\Delta S_D(\tau) := S_D(\rho(\tau); H(\lambda_\tau)) - S_D(\rho(0); H(\lambda_0)), \tag{61}$$

$$\mathcal{W}_q^D := \mathcal{W}_q\big(\rho_{\mathcal{C}_{H(\lambda_\tau)}}(\tau), \rho(0)\big). \tag{62}$$

Substituting $\mathcal{C}^i = \mathcal{C}_{H(\lambda_0)}$ and $\mathcal{C}^f = \mathcal{C}_{H(\lambda_\tau)}$ into the general inequality, we obtain

$$\Delta S_D(\tau) \geqslant 2\big(\mathcal{W}_q^D\big)^2. \tag{63}$$

Equivalently, by introducing the average diagonal entropy-production rate

$$\bar{\sigma}_D(\tau) := \frac{\Delta S_D(\tau)}{\tau}, \tag{64}$$

we obtain the thermodynamic speed-limit inequality

$$\tau \geqslant \frac{2\big(\mathcal{W}_q^D\big)^2}{\bar{\sigma}_D(\tau)} =: \tau_D. \tag{65}$$

This inequality bounds how fast a driven isolated system can change its occupation distribution in the energy eigenbasis

at a fixed rate of diagonal entropy production. It is therefore directly relevant to irreversibility under time-dependent Hamiltonians, including quantum quenches and shortcuts to adiabaticity.

V. APPLICATIONS

A. Hydrodynamic-mode relaxation

To illustrate FOE's bound (56), we consider the unitary dynamics of the mixed-field Ising chain

$$H = -J\sum_{i=1}^{L}\sigma_i^z\sigma_{i+1}^z - h_x\sum_{i=1}^{L}\sigma_i^x - h_z\sum_{i=1}^{L}\sigma_i^z, \tag{66}$$

with periodic boundary conditions. For nonzero J, h_x, and h_z, this model is a simple nonintegrable spin chain. The initial state is chosen as a product of local Gibbs states,

$$\rho(0) = \bigotimes_{i=1}^{L}\frac{e^{-\beta_i H_{\rm loc}}}{Z_i}, \quad H_{\rm loc} = -h_x\sigma^x - h_z\sigma^z, \tag{67}$$

where the inverse temperatures are given by $\beta_i = 1/T_i$, with the site-dependent temperature prepared as a Gaussian profile,

$$T_i = 10 + 10\exp\left[-\frac{5\left(i-\frac{L+1}{2}\right)^2}{2L^2}\right]. \tag{68}$$

The state evolves unitarily as

$$\rho(t) = e^{-iHt}\rho(0)e^{iHt}. \tag{69}$$

We use the local-energy coarse graining defined by the product eigenbasis of $H_{\rm loc}$.

Figure 3 shows $\Delta S_{\rm FOE}(t)$ and $2(\mathcal{W}_q^{\rm FOE}(t))^2$. The numerical result confirms that the entropy production is bounded from below by the Wasserstein term throughout the evolution. As shown in Fig. 3(a), both quantities start from zero, increase during the initial relaxation, and then approach a slowly varying plateau with finite-size fluctuations. This similarity reflects the fact that both quantities are determined by the same coarse-grained local-energy distribution. The behavior of $2(\mathcal{W}_q^{\rm FOE}(t))^2$ therefore suggests that the VS-QW captures information about the coarse-grained local-energy profile in this finite-size example.

Figure 3(b) shows the speed-limit lower bound obtained from FOE entropy production. The bound remains below the actual elapsed time $J\tau$, confirming the FOE speed limit throughout the unitary relaxation dynamics. Since the lower bound is finite, the local-energy macrostate cannot change in an arbitrarily short time at a fixed average FOE entropy-production rate. The gap between the bound and the actual time is partly due to the fact that the VS-QW used here is an $O(1)$ quantity, bounded independently of system size. Nevertheless, the bound remains nontrivial for the finite system considered here. The oscillatory behavior reflects finite-size coherent dynamics rather than purely monotonic hydrodynamic diffusion.

B. Shortcuts to adiabaticity

The inequalities presented in Sec. IV show that, in isolated quantum systems, fast state transformations can incur

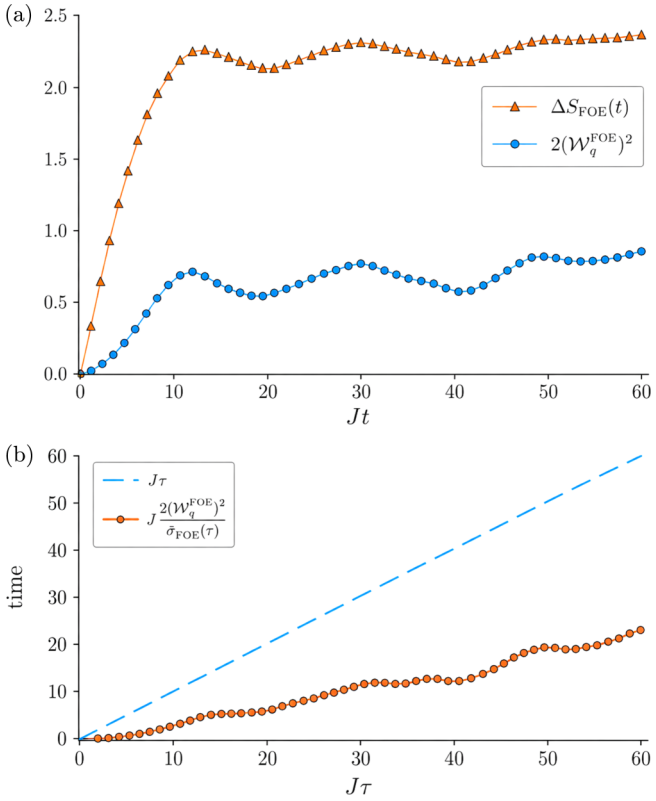


FIG. 3. In panel (a), time evolution of the FOE observational entropy production $\Delta S_{\rm FOE}(t)$ and the Wasserstein-distance bound $2(\mathcal{W}_q^{\rm FOE})^2$. In panel (b), thermodynamic speed-limit bound for the FOE relaxation dynamics. The blue dashed line shows the actual elapsed time $J\tau$, while the orange circles show right-hand side of Eq. (58). The orange curve stays below the blue dashed line, confirming the speed-limit inequality. The horizontal axis is Jt, and the vertical axis shows the value multiplied by 10^3. Here, $L = 10$, $h_x = 1.0$, $h_z = 1.1$, and $J = 0.01$.

nonadiabatic costs such as Gibbs entropy production and diagonal entropy production. A primary example of fast state transformations in isolated systems is quantum computation. In particular, there is an implementation scheme known as adiabatic quantum computation. The computation is carried out by adiabatically evolving the system from the ground state of an initial Hamiltonian, whose ground state can be prepared easily, to the ground state of a final Hamiltonian whose ground state encodes the solution of the problem of interest. Although adiabatic transformations typically require infinitely long operation times, a variety of techniques collectively known as STA have been developed to implement them within finite time. Among the various STA methods proposed in the literature, we explain how our main result can be applied to shortcuts to adiabaticity by taking counterdiabatic (CD) driving [44,45] as a concrete example.

Counterdiabatic driving is a method for achieving adiabatic transformations within finite time in isolated quantum systems. For example, consider the case where the ground state $|0(\lambda_0)\rangle$ of the system Hamiltonian $H_0(\lambda_0)$ is driven by external control so that it evolves into the ground state $|0(\lambda_\tau)\rangle$ of $H_0(\lambda_\tau)$. However, in general, this type of operation can only be carried out in the quasistatic driving, and thus requires an

infinitely long operation time. In counterdiabatic driving, one introduces an additional Hamiltonian that suppresses diabatic transitions,

$$H_1(\lambda_t) := i\frac{\mathrm{d}\lambda}{\mathrm{d}t}\sum_n (|\partial_\lambda n\rangle\langle n| - \langle n|\partial_\lambda n\rangle|n\rangle\langle n|), \tag{70}$$

and modifies the system Hamiltonian to counterdiabatic Hamiltonian $H_0(\lambda_t) + H_1(\lambda_t)$. Here, $|n\rangle$ denotes the eigenstates of H_0 and $|\partial_\lambda n\rangle := \partial_\lambda |n\rangle$. With this modification, the quantum state undergoes adiabatic evolution even when λ_t is varied rapidly.

From a thermodynamic perspective, it is natural to expect that performing an operation more rapidly entails a thermodynamic cost. However, STA protocols such as counterdiabatic driving appear to realize finite-time adiabatic operations without end-point entropy production. This is because, at the end of the protocol [i.e., when $H_1(\lambda_\tau) = 0$], the population distribution over the energy eigenstates is identical to that of the initial state. Consequently, the entropy production vanishes both for the Gibbs entropy and for the diagonal entropy. Therefore, whether a thermodynamic cost associated with the operation time of counterdiabatic driving exists is a nontrivial and important question. Previous studies [46,47] have addressed the relation between the operation time and the cost of counterdiabatic driving, but its connection to entropy—the most fundamental quantity characterizing thermodynamic cost—has remained unclear. From Eqs. (34), (36), and (65), we obtain the following inequalities for the operation time τ of any STA protocol, including counterdiabatic:

$$\tau_{\max,2} := \ln 2 \max_{0\leqslant t\leqslant\tau} \frac{\mathcal{W}_q\big(\rho_{\mathcal{C}_{H(\lambda_t)}}(t), \rho(0)\big)^2}{\langle\sigma_G\rangle_t} \leqslant \tau, \tag{71}$$

$$\tau_{\max,1} := \ln\left(\frac{d}{d-1}\right) \max_{0\leqslant t\leqslant\tau} \frac{\mathcal{W}_q\big(\rho_{\mathcal{C}_{H(\lambda_t)}}(t), \rho(0)\big)}{\langle\sigma_G\rangle_t} \leqslant \tau, \tag{72}$$

$$\tau_{\max} := 2 \max_{0\leqslant t\leqslant\tau} \frac{\mathcal{W}_q\big(\rho_{\mathcal{C}_{H(\lambda_t)}}(t), \rho(0)\big)^2}{\langle\sigma_D\rangle_t} \leqslant \tau. \tag{73}$$

These results follow immediately from the fact that the maxima on the right-hand sides of Eqs. (71)–(73) are attained at times smaller than τ.

We explain the meaning of these inequalities. As a remark, the state $\rho_{\mathcal{C}_{H(\lambda_\tau)}}(\tau)$ appearing in Eqs. (71)–(73) is the projected state not with respect to the original Hamiltonian $H_0(\lambda_t)$, but with respect to the Hamiltonian under STA, such as $H_0(\lambda_t) + H_1(\lambda_t)$. Under the present coarse-grained definition of entropy production, these equations imply that a finite-time STA protocol cannot keep the time-averaged entropy-production rate zero at all intermediate times whenever the intermediate energy-diagonal state is separated from the initial state by a finite VS-QW distance. This is because, along the protocol, there necessarily exists a time $t \in [0, \tau)$ such that $\mathcal{W}_q(\rho_{\mathcal{C}_{H(\lambda_\tau)}}(\tau), \rho(0)) > 0$, since $\rho_{\mathcal{C}_{H(\lambda_\tau)}}(\tau)$ corresponds to the quantum state evolving adiabatically at intermediate times. Assuming that the STA protocol is completed at time τ, this implies that $\langle\sigma_D\rangle_t > 0$ must hold.

We next numerically demonstrate Eqs. (71)–(73) using a finite-time Landau-Zener process assisted by a counterdiabatic protocol [48]. The counterdiabatic Hamiltonian of this system is given by

$$H(t) = bt\sigma_z + \sigma_x - \frac{b}{2+2(bt)^2}\sigma_y, \tag{74}$$

$$H_0(t) := bt\sigma_z + \sigma_x, \tag{75}$$

where

$$\sigma_x = \begin{pmatrix} 0 & 1 \\ 1 & 0 \end{pmatrix}, \quad \sigma_y = \begin{pmatrix} 0 & i \\ -i & 0 \end{pmatrix}, \quad \sigma_z = \begin{pmatrix} 1 & 0 \\ 0 & -1 \end{pmatrix}. \tag{76}$$

Here, $H_0(t)$ represents the Hamiltonian of the Landau-Zener process, while the term $-b\sigma_y/\{2 + 2(bt)^2\}$ corresponds to the counterdiabatic correction. The operation considered in our numerical calculation consists of the following four steps:

(1) For time $t \in [-\infty, -b^{-1}]$, the Hamiltonian is fixed as $H_0(-b^{-1}) = -\sigma_z + \sigma_x$.

(2) At $t = -b^{-1}$, we perform a quench to change the Hamiltonian to $H_0(-b^{-1}) - \frac{b}{4}\sigma_y$.

(3) For time $t \in (-b^{-1}, b^{-1})$, the Hamiltonian of the system is given by $H(t)$.

(4) At time $t = b^{-1}$, we perform another quench, changing the Hamiltonian to $H_0(b^{-1}) = \sigma_z + \sigma_x$, after which the operation is terminated.

In this operation, b determines the operation speed. In the numerical simulations, we varied b and investigated the bounds in Eqs. (71)–(73). The initial state was chosen as

$$\rho = \tfrac{9}{10}|0\rangle\langle 0| + \tfrac{1}{10}|1\rangle\langle 1|, \tag{77}$$

where $|0\rangle$ and $|1\rangle$ denote the ground and excited states of $H_0(-b^{-1})$, respectively.

In Fig. 4, the dots represent the right-hand sides of Eqs. (71)–(73), while the solid line $y = \tau$ is shown as a reference. As seen in the figure, for the same operation, the right-hand sides of the inequalities (71)–(73) increase monotonically as the operation speed is decreased.

The saturation of the linear Gibbs-entropy bound in Eq. (36) for the present two-level example can be understood as follows. Let $p_t = (p_g(t), p_e(t))$ be the population distribution of the energy-diagonal state $\rho_{H(\lambda_t)}(t)$. $p_e(t)$ denotes the excited-state population. For a two-level system, the Gibbs entropy of the energy-diagonal state is given by $S_G(\rho_{\mathcal{C}_{H(\lambda_\tau)}}(\tau), H(t)) = (\ln 2)p_e(t)$. Since the initial state is passive, the induced doubly stochastic transition gives $p_e(t) \geqslant p_e(0)$, and hence the Gibbs entropy production becomes

$$\Delta S_G(t) = (\ln 2)[p_e(t) - p_e(0)] = (\ln 2)d_{\mathrm{TV}}(p_t, p_0), \tag{78}$$

where $d_{\mathrm{TV}}(p_t, p_0) = \frac{1}{2}|p_t - p_0|_1$. Moreover, as long as $p_e(t) < 1/2$, the ordering of the eigenvalues is unchanged. Therefore, the closed-form expression of the Vu-Saito quantum Wasserstein distance gives

$$W_q^G = d_{\mathrm{TV}}(p_t, p_0). \tag{79}$$

Combining these relations, we obtain

$$\Delta S_G(t) = (\ln 2)W_q^D, \tag{80}$$

which shows that the linear bound in Eq. (36) is saturated.

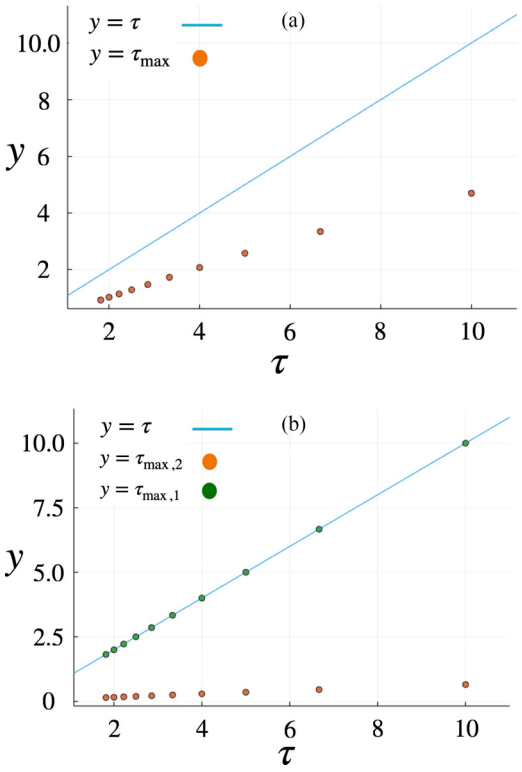


FIG. 4. A plot of the LZ CD protocol. We simulated the dynamics of a two-level system driven from the initial Hamiltonian $-10\sigma_z + \sigma_x$ to $10\sigma_z + \sigma_x$ with a counterdiabatic term included, over the time interval $t \in [-t_0, t_0]$, with $t_0 = 10b^{-1}$. The parameter b was varied from 10^3 to 10^4 in increments of 10^3. The horizontal axis shows the operation time, rescaled by a factor of 10^3. The vertical axis shows the values of the left- and right-hand sides of inequalities [Eqs. (71)–(73)], also rescaled by 10^3. In panel (a), the orange dots represent the simulated data corresponding to Eq. (73). In panel (b), the orange dots represent the simulated data corresponding to Eq. (71), while the green dots represent the simulated data corresponding to Eq. (72).

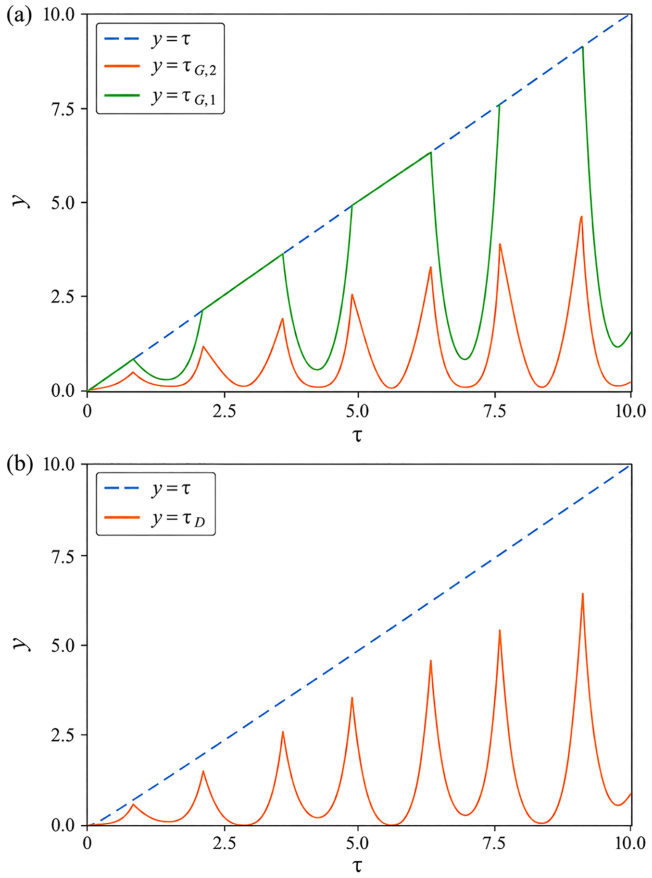


FIG. 5. Speed-limit bounds for the Rabi-cycle model. The blue dashed line denotes the actual operation time $y = \tau$. (a) Gibbs-entropy bounds $y = \tau_{G,2}$ and $y = \tau_{G,1}$. (b) Diagonal-entropy bound $y = \tau_D$. All speed-limit curves lie at or below $y = \tau$, confirming the thermodynamic speed-limit inequalities throughout the dynamics.

C. Rabi cycle: solvable model

This example mainly serves as an analytically solvable consistency check of the general bounds.

We demonstrate our results [Eqs. (32), (34)–(36), (63), and (65)]. Using the analytical expressions obtained below, we illustrate the thermodynamic speed-limit inequalities [Eqs. (34), (36), and (65)] in Fig. 5 and the generalized second-law inequalities [Eqs. (32), (35), and (63)] in Fig. 6. We consider the two-level Hamiltonian

$$H(t) = \sigma_z + b\cos(\omega t)\sigma_x + b\sin(\omega t)\sigma_y. \tag{81}$$

We define

$$\Omega = \sqrt{\left(1 - \frac{\omega}{2}\right)^2 + b^2}, \quad \Omega_0 = \sqrt{1 + b^2}. \tag{82}$$

The initial state is chosen as the ground state of $H(0) = \sigma_z + b\sigma_x$, namely,

$$\rho(0) = |g(0)\rangle\langle g(0)|. \tag{83}$$

Then, the excitation probability with respect to the instantaneous energy eigenbasis of $H(t)$ is given by

$$P_e(t) = \frac{b^2\omega^2}{4(1+b^2)\left[\left(1 - \frac{\omega}{2}\right)^2 + b^2\right]}\sin^2(\Omega t). \tag{84}$$

VS-QW becomes

$$W_q(\rho_{\mathrm{D}}(t), \rho(0)) = \frac{1 - |2P_e(t) - 1|}{2}. \tag{85}$$

The Gibbs entropy production is

$$\Delta S_G(t) = (\ln 2)P_e(t), \tag{86}$$

whereas the diagonal entropy production is

$$\Delta S_{\mathrm{D}}(t) = -P_e(t)\ln P_e(t) - (1 - P_e(t))\ln(1 - P_e(t)). \tag{87}$$

We find

$$\Delta S_G(t) = (\ln 2)W_q(t), \quad \text{for} \quad P_e(t) \leqslant \tfrac{1}{2}. \tag{88}$$

Thus, the linear Gibbs bound is saturated before the eigenvalue-exchange point

$$P_e(t) = \tfrac{1}{2}. \tag{89}$$

After this point, the Wasserstein distance folds back, while $\Delta S_G(t)$ remains proportional to $P_e(t)$.

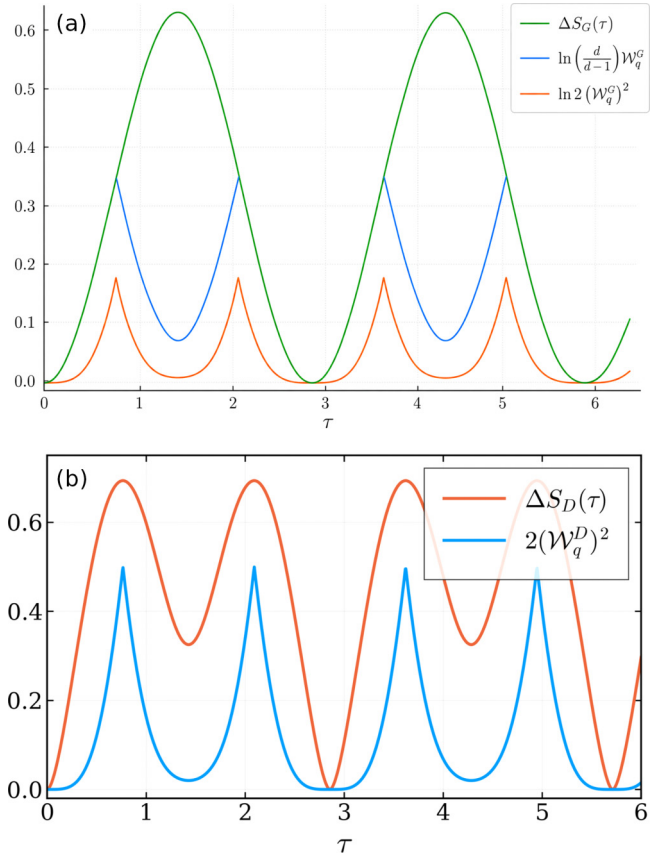


FIG. 6. Entropy production and Wasserstein-distance lower bounds in the Rabi-cycle model. (a) Gibbs entropy production $\Delta S_G(\tau)$ together with $\ln(d/(d-1))\mathcal{W}_q^G$ and $\ln 2\,(\mathcal{W}_q^G)^2$. (b) Diagonal entropy production $\Delta S_D(\tau)$ together with $2(\mathcal{W}_q^D)^2$.

We briefly discuss the short-time behavior of the quantities introduced above. Since

$$\sin^2(\Omega t) = \Omega^2 t^2 + O(t^4), \tag{90}$$

the excitation probability behaves as

$$P_e(t) = \gamma t^2 + O(t^4), \quad \gamma := \frac{b^2\omega^2}{4(1+b^2)}. \tag{91}$$

Thus, for sufficiently short times, one has

$$P_e(t) < \tfrac{1}{2}. \tag{92}$$

In this regime, the ordered eigenvalues of the energy-diagonal state are not exchanged, and the Vu-Saito quantum Wasserstein distance is simply

$$W_q(t) = P_e(t) = \gamma t^2 + O(t^4). \tag{93}$$

The Gibbs entropy production therefore grows quadratically in time:

$$\Delta S_G(t) = (\ln 2) P_e(t) = (\ln 2)\gamma t^2 + O(t^4). \tag{94}$$

In particular, the linear Gibbs bound is saturated in the short-time regime:

$$\Delta S_G(t) = (\ln 2) W_q(t) + O(t^4). \tag{95}$$

On the other hand, the quadratic Gibbs bound behaves as

$$(\ln 2) W_q(t)^2 = (\ln 2)\gamma^2 t^4 + O(t^6). \tag{96}$$

Hence, the linear Gibbs bound captures the correct short-time scaling, whereas the quadratic Gibbs bound is subleading.

The diagonal entropy production has a different short-time structure because of the logarithmic singularity of the Shannon entropy near a pure state. Using

$$-p\ln p - (1-p)\ln(1-p) = p(1-\ln p) + O(p^2), \tag{97}$$

with

$$p = P_e(t), \tag{98}$$

we obtain

$$\Delta S_{\mathrm{D}}(t) = \gamma t^2[1 - \ln(\gamma t^2)] + O(t^4|\ln t|). \tag{99}$$

Therefore, the diagonal entropy production is larger than a purely quadratic function by the logarithmic factor

$$|\ln t|. \tag{100}$$

The corresponding lower bound behaves as

$$2W_q(t)^2 = 2\gamma^2 t^4 + O(t^6). \tag{101}$$

Thus, for short times, the diagonal-entropy bound is much weaker than the actual diagonal entropy production. This difference originates from the nonanalytic behavior of the Shannon entropy at the initial pure state.

VI. DERIVATIONS OF MAIN RESULTS

First, we show the derivation of Eq. (40).

Proof. We first recall the definitions used below. Let $\mathcal{C} = \{\hat{P}_x\}_x$ be a PVM on a d-dimensional Hilbert space, namely,

$$\hat{P}_x \geqslant 0, \quad \hat{P}_x\hat{P}_y = \delta_{xy}\hat{P}_x, \quad \sum_x \hat{P}_x = \hat{1}. \tag{102}$$

For a state ρ, the observational entropy associated with $\mathcal{C}$ is defined by

$$S_{\mathrm{obs}}^{\mathcal{C}}(\rho) := -\sum_x p_x \ln\frac{p_x}{V_x}, \quad p_x := \mathrm{tr}[\hat{P}_x\rho], \quad V_x := \mathrm{tr}[\hat{P}_x]. \tag{103}$$

We say that ρ is macroscopic with respect to $\mathcal{C}$ if $S_{\mathrm{obs}}^{\mathcal{C}}(\rho) = S_{\mathrm{vN}}(\rho)$. Equivalently, ρ is of the form

$$\rho = \rho_{\mathcal{C}} := \sum_x p_x \frac{\hat{P}_x}{V_x}. \tag{104}$$

In the following, we consider an initial PVM $\mathcal{C}^0 = \{\hat{P}_y^0\}_y$, a final PVM $\mathcal{C}^t = \{\hat{P}_x^t\}_x$, and a unitary evolution $\rho_t = \hat{U}\rho_0\hat{U}^\dagger$. We assume that the initial state is macroscopic with respect to $\mathcal{C}^0$, i.e.,

$$\rho_0 = \rho_{\mathcal{C}^0} = \sum_y p_y(0)\frac{\hat{P}_y^0}{V_y^0}. \tag{105}$$

The final coarse-grained state is

$$\rho_{\mathcal{C}^t}(t) = \sum_x p_x(t)\frac{\hat{P}_x^t}{V_x^t}, \quad p_x(t) := \mathrm{tr}\big[\hat{P}_x^t\rho_t\big], \quad V_x^t := \mathrm{tr}\big[\hat{P}_x^t\big]. \tag{106}$$

We now rewrite the observational entropies as Shannon entropies of microscopic probability vectors. For each macrospace x, introduce V_x^t microscopic labels $i \in x$ and define

$$q_i(t) := \frac{p_x(t)}{V_x^t} \quad (i \in x). \tag{107}$$

Similarly, for $j \in y$, define

$$q_j(0) := \frac{p_y(0)}{V_y^0}. \tag{108}$$

Then,

$$S_{\mathrm{obs}}^{\mathcal{C}^t}(\rho_t) = -\sum_i q_i(t) \ln q_i(t), \tag{109}$$

$$S_{\mathrm{obs}}^{\mathcal{C}^0}(\rho_0) = -\sum_j q_j(0) \ln q_j(0). \tag{110}$$

We next show that $q(t)$ is obtained from $q(0)$ by a doubly stochastic matrix. Indeed, for $i \in x$,

$$\begin{aligned} q_i(t) &= \frac{1}{V_x^t} \mathrm{tr}\big[\hat{P}_x^t \hat{U} \rho_0 \hat{U}^\dagger\big] = \sum_y \frac{\mathrm{tr}\big[\hat{U}^\dagger \hat{P}_x^t \hat{U} \hat{P}_y^0\big]}{V_x^t V_y^0} p_y(0) \\ &= \sum_y \sum_{j \in y} \frac{\mathrm{tr}\big[\hat{U}^\dagger \hat{P}_x^t \hat{U} \hat{P}_y^0\big]}{V_x^t V_y^0} q_j(0). \end{aligned} \tag{111}$$

Thus, if $i \in x$ and $j \in y$, we define

$$B_{ij} := \frac{\mathrm{tr}\big[\hat{U}^\dagger \hat{P}_x^t \hat{U} \hat{P}_y^0\big]}{V_x^t V_y^0}; \tag{112}$$

then,

$$q_i(t) = \sum_j B_{ij} q_j(0). \tag{113}$$

The matrix B is non-negative, because

$$\begin{aligned} B_{ij} V_x^t V_y^0 &= \mathrm{tr}\big[\sqrt{P_y^0} \hat{U}^\dagger \hat{P}_x^t \hat{U} \sqrt{\hat{P}_y^0}\big] \\ &= \mathrm{tr}\big[\big(\sqrt{P_y^0} \hat{U}^\dagger \sqrt{\hat{P}_x^t}\big)\big(\sqrt{P_y^0} \hat{U} \sqrt{\hat{P}_x^t}\big)^\dagger\big] \geqslant 0. \end{aligned} \tag{114}$$

Moreover,

$$\sum_i B_{ij} = \sum_x \sum_{i \in x} \frac{\mathrm{tr}\big[\hat{U}^\dagger \hat{P}_x^t \hat{U} \hat{P}_y^0\big]}{V_x^t V_y^0} = \sum_x \frac{\mathrm{tr}\big[\hat{U}^\dagger \hat{P}_x^t \hat{U} \hat{P}_y^0\big]}{V_y^0} = 1 \tag{115}$$

and

$$\sum_j B_{ij} = \sum_y \sum_{j \in y} \frac{\mathrm{tr}\big[\hat{U}^\dagger \hat{P}_x^t \hat{U} \hat{P}_y^0\big]}{V_x^t V_y^0} = \sum_y \frac{\mathrm{tr}\big[\hat{U}^\dagger \hat{P}_x^t \hat{U} \hat{P}_y^0\big]}{V_x^t} = 1. \tag{116}$$

Therefore, B is doubly stochastic.

Let $Q(0)$ and $Q(t)$ be the probability vectors obtained by rearranging $q(0)$ and $q(t)$ in nonincreasing order. Since permutations are also doubly stochastic, the transition from $Q(0)$ to $Q(t)$ is again described by a doubly stochastic matrix. Hence, $Q(0)$ majorizes $Q(t)$. Using the Lenard-Tasaki inequality in Appendix E, we obtain

$$\begin{aligned} &S_{\mathrm{obs}}^{\mathcal{C}^t}(\rho_t) - S_{\mathrm{obs}}^{\mathcal{C}^0}(\rho_0) \\ &\quad = -\sum_i Q_i(t) \ln Q_i(t) + \sum_i Q_i(0) \ln Q_i(0) \\ &\quad = D(Q(0)\|Q(t)) + \sum_i (Q_i(0) - Q_i(t)) \ln Q_i(t) \\ &\quad \geqslant D(Q(0)\|Q(t)). \end{aligned} \tag{117}$$

Here,

$$D(Q(0)\|Q(t)) := \sum_i Q_i(0) \ln \frac{Q_i(0)}{Q_i(t)} \tag{118}$$

is the classical relative entropy. Applying Pinsker's inequality gives

$$S_{\mathrm{obs}}^{\mathcal{C}^t}(\rho_t) - S_{\mathrm{obs}}^{\mathcal{C}^0}(\rho_0) \geqslant \tfrac{1}{2} \|Q(t) - Q(0)\|_1^2. \tag{119}$$

It remains to identify this classical distance with VS-QW. The eigenvalue lists of $\rho_{\mathcal{C}^t}(t)$ and $\rho_{\mathcal{C}^0}(0)$ are precisely $Q(t)$ and $Q(0)$, respectively. Therefore, by the closed form of VS-QW (see Appendix C),

$$\mathcal{W}_q(\rho_{\mathcal{C}^t}(t), \rho_{\mathcal{C}^0}(0)) = \tfrac{1}{2} \|Q(t) - Q(0)\|_1. \tag{120}$$

Consequently,

$$S_{\mathrm{obs}}^{\mathcal{C}^t}(\rho_t) - S_{\mathrm{obs}}^{\mathcal{C}^0}(\rho_0) \geqslant 2\mathcal{W}_q(\rho_{\mathcal{C}^t}(t), \rho_{\mathcal{C}^0}(0))^2. \tag{121}$$

This proves the desired entropy-production bound. ■

Next, we show the derivation of Eqs. (32) and (35).

Proof. Let the spectral decompositions of the initial and final Hamiltonians be

$$\begin{aligned} \hat{H}(\lambda_0) &= \sum_{i=1}^{n_0} E_i(\lambda_0) \hat{P}_i^{(E)}(\lambda_0), \\ \hat{H}(\lambda_\tau) &= \sum_{i=1}^{n_\tau} E_i(\lambda_\tau) \hat{P}_i^{(E)}(\lambda_\tau). \end{aligned} \tag{122}$$

For the initial and final states $\rho(0)$ and $\rho(\tau)$, consider classical probability distributions $p, q \in \mathbb{R}^d$ whose ith components are

$$p_i = \frac{\mathrm{tr}\big[\hat{P}_i^{(E)}(\lambda_0)\rho(0)\big]}{\mathrm{tr}\big[\hat{P}_i^{(E)}(\lambda_0)\big]}, \quad q_i = \frac{\mathrm{tr}\big[\hat{P}_i^{(E)}(\lambda_\tau)\rho(\tau)\big]}{\mathrm{tr}\big[\hat{P}_i^{(E)}(\lambda_\tau)\big]}. \tag{123}$$

As in the case of observational entropy, the matrix B describing the time evolution from $\{p_i\}_i$ to $\{q_i\}_i$, defined by

$$B_{ij} = \frac{\mathrm{tr}\big[\hat{U}^\dagger \hat{P}_i^{(E)}(\lambda_\tau) \hat{U} \hat{P}_j^{(E)}(\lambda_0)\big]}{\mathrm{tr}\big[\hat{P}_j^{(E)}(\lambda_0)\big] \mathrm{tr}\big[\hat{P}_i^{(E)}(\lambda_\tau)\big]}, \tag{124}$$

is a doubly stochastic matrix. Birkhoff–von Neumann theorem [49] states that any doubly stochastic matrix can be expressed as a convex combination of permutation matrices. Accordingly, we represent B as $B = \sum_a c_a R_a$, where c_a is a discrete probability distribution and R_a are permutation matrices.

Next, let $x \in \mathbb{R}^d$ and consider the following functions:

$$V_1(x) := \sum_{n=1}^{d} \ln n(x_n - p_n) - \frac{1}{2} \ln\left(\frac{d}{d-1}\right) \|x - p\|_1, \tag{125}$$

$$V_2(x) := \sum_{n=1}^{d} \ln n(x_n - p_n) - \frac{\ln 2}{4}\|x-p\|_1^2. \tag{126}$$

Here, $\|x-p\|_1 = \sum_n |x_n - p_n|$. Since the first term of $V_1(x), V_2(x)$ is concave and the second terms are convex, it follows that $V_1(x), V_2(x)$ are concave. A function $f : \mathbb{R}^d \to \mathbb{R}$ is said to be concave if it satisfies the following condition: $\forall x, y \in \mathbb{R}^d, \forall \lambda \in [0,1]$,

$$f(\lambda x + (1-\lambda)y) \geqslant \lambda f(x) + (1-\lambda) f(y). \tag{127}$$

Therefore, we obtain

$$V_i(Tp) \geqslant \sum_a c_a V_i(R_a p) \quad (i = 1, 2). \tag{128}$$

Focus on one permutation matrix R_a contained in B. If R_a permutes the nth and mth components with $n > m$; then, we obtain

$$V_1(R_a p) = (p_m - p_n)\left\{\ln\frac{n}{m} - \ln\left(\frac{d}{d-1}\right)\right\}, \tag{129}$$

$$V_2(R_a p) = (p_m - p_n)\left(\ln\frac{n}{m} - \ln 2(p_m - p_n)\right). \tag{130}$$

Since $p_m \geqslant p_n$, the signs of $V_1(R_a p)$ and $V_2(R_a p)$ are determined by $\ln(n/m) - \ln\{d/(d-1)\}$ and $\ln(n/m) - (\ln 2)(p_m - p_n)$, respectively. Because $\ln(n/m) \geqslant \ln\{(m+1)/m\} \geqslant \ln\{d/(d-1)\}$, we obtain $V_1(R_a p) \geqslant 0$. From the passivity of $\rho(0)$ and normalization constant, one has $1/m \geqslant p_m$; together with $n > m$, this implies

$$\ln\frac{n}{m} - \ln 2(p_m - p_n) \geqslant \ln\frac{m+1}{m} - \ln 2\frac{1}{m}. \tag{131}$$

The right-hand side of Eq. (131) is positive for $m > 0$, as can be verified by a straightforward calculation. Combining Eqs. (128)–(131), we obtain $V_1(Tp) \geqslant 0, V_2(Tp) \geqslant 0$. Therefore, we obtain

$$S_G(\rho(\tau), \lambda_\tau) - S_G(\rho(0), \lambda_0) \geqslant \frac{1}{2}\ln\left(\frac{d}{d-1}\right)\|q-p\|_1, \tag{132}$$

$$S_G(\rho(\tau), \lambda_\tau) - S_G(\rho(0), \lambda_0) \geqslant \frac{\ln 2}{4}\|q-p\|_1^2. \tag{133}$$

Next, we relate the classical distance $\|q-p\|_1$ to the Vu-Saito quantum Wasserstein distance. We consider a unitary U that maps the nth energy eigenstate of $H(\lambda_\tau)$ to the nth energy eigenstate of $H(\lambda_0)$. If degeneracies are present, we use an arbitrarily fixed orthonormal basis in each degenerate eigenspace. Then, we have

$$\tfrac{1}{2}\|q-p\|_1 = \tfrac{1}{2}\|U\rho_{H(\lambda_\tau)}(\tau)U^\dagger - \rho(0)\|_1. \tag{134}$$

By the definition of the Vu-Saito quantum Wasserstein distance, we further obtain

$$\begin{aligned}\tfrac{1}{2}\|q-p\|_1 &= \tfrac{1}{2}\left\|U\rho_{H(\lambda_\tau)}(\tau)U^\dagger - \rho(0)\right\|_1 \\ &\geqslant \mathcal{W}_q\left(U\rho_{H(\lambda_\tau)}(\tau)U^\dagger, \rho(0)\right).\end{aligned} \tag{135}$$

We conclude from the above that

$$S_G(\rho(\tau), \lambda_\tau) - S_G(\rho(0), \lambda_0) \geqslant \ln\frac{d}{d-1}\mathcal{W}_q(\rho_D(\tau), \rho(0)), \tag{136}$$

$$S_G(\rho(\tau), \lambda_\tau) - S_G(\rho(0), \lambda_0) \geqslant \ln 2\mathcal{W}_q(\rho_D(\tau), \rho(0))^2. \tag{137}$$

■

VII. CONCLUDING REMARKS AND OUTLOOKS

In this work, we derived thermodynamic speed limits for isolated quantum systems undergoing finite-time unitary dynamics. Since the von Neumann entropy is conserved under unitary evolution, thermodynamic irreversibility must be formulated at the level of coarse-grained descriptions. We showed that entropy production associated with the Gibbs entropy and with several thermodynamically motivated observational entropies is bounded from below by the Vu-Saito quantum Wasserstein distance between the initial and final coarse-grained states. Dividing these generalized second-law inequalities by the average entropy-production rate gives lower bounds on the operation time.

The resulting bounds clarify a thermodynamic aspect of speed limits in isolated quantum systems. Ordinary quantum speed limits constrain the operation time by kinematic quantities, such as Hilbert-space distances and energetic fluctuations. In contrast, the bounds derived here constrain the operation time by the entropic cost required to change a thermodynamic macrostate. They therefore quantify the statement that a finite change of a coarse-grained state cannot be achieved in an arbitrarily short time under a fixed entropy-production rate. We also note that the present lower bounds are complementary to standard continuity bounds for entropy. Since observational entropy is the von Neumann entropy of the corresponding coarse-grained state, Fannes-Audenaert-type inequalities [31,50–52] give upper bounds

$$\Delta S_{\mathcal{C}^i \to \mathcal{C}^f}(\tau) \leqslant T\log_2(d-1) + H((T, 1-T)) \tag{138}$$

on the entropy production in terms of the trace distance $T = \frac{1}{2}\|\rho_{\mathcal{C}^f}(\tau) - \rho_{\mathcal{C}^i}(0)\|_1$ between the initial and final coarse-grained states. Here, $H((p, 1-p))$ denotes the binary entropy function. Thus, coarse-grained entropy production is constrained from both below and above by distances between macroscopic states.

A central open problem is to construct an extensive version of the quantum Wasserstein distance suitable for macroscopic systems. The Vu-Saito distance used here is an $O(V^0)$ quantity, so the present lower bounds may become weak when entropy production scales extensively with system size. Developing hydrodynamic or extensive quantum transport distances would turn the finite-dimensional inequalities derived here into thermodynamically robust speed limits for macroscopic isolated quantum systems. Another important direction is to clarify how the present isolated-system bounds reduce to, or differ from, known open-system speed limits under weak-coupling, large-bath, or Markovian limits.

ACKNOWLEDGMENTS

R.K. is grateful to K. Saito for his continuous discussions and encouragement. We thank K. Yokota, M. Itami, and K. Tamano for careful reading of the manuscript and

helpful comments. This study was supported by JST SPRING Grant No. JPMJSP2110 and JSPS KAKENHI Grants No. JP26H02015 and No. JP26H00388.

DATA AVAILABILITY

The data that support the findings of this article are not publicly available upon publication because it is not technically feasible and/or the cost of preparing, depositing, and hosting the data would be prohibitive within the terms of this research project. The data are available from the authors upon reasonable request.

APPENDIX A: THERMODYNAMIC COARSE GRAININGS

In this Appendix, we provide detailed definitions and physical interpretations of the thermodynamic coarse grainings introduced in the main text. We consider the system-bath, local-energy, and global-energy coarse grainings. We also derive the relation between the system-bath observational entropy and the conventional entropy production of an open quantum system.

1. System-bath coarse graining

Consider a small system S interacting with a large bath B. The total Hamiltonian is

$$H(\lambda) = H_S(\lambda) \otimes I_B + I_S \otimes H_B + H_I, \tag{A1}$$

where H_I denotes the interaction Hamiltonian. The projector onto the jth bath-energy mesoscopic window and its volume are defined by

$$\Pi_j^B := \mathbf{1}_j(H_B), \quad \Omega_j^B := \mathrm{tr}_B\big[\Pi_j^B\big]. \tag{A2}$$

For a total state ρ, let

$$\rho_S := \mathrm{tr}_B[\rho] = \sum_i \nu_i \hat{P}_i^{(\rho_S)} \tag{A3}$$

be the spectral decomposition of the reduced-system state. The projector onto the kernel of ρ_S is included in $\{\hat{P}_i^{(\rho_S)}\}_i$ when necessary. We define the state-dependent coarse graining

$$\mathcal{C}_{\rho,H_B} := \big\{\hat{P}_i^{(\rho_S)} \otimes \Pi_j^B\big\}_{ij}. \tag{A4}$$

The corresponding probabilities and subspace dimensions are

$$p_{ij} := \mathrm{tr}\big[(\hat{P}_i^{(\rho_S)} \otimes \Pi_j^B)\rho\big], \tag{A5}$$

$$d_i := \mathrm{tr}_S\big[\hat{P}_i^{(\rho_S)}\big]. \tag{A6}$$

The associated observational entropy is

$$S_{\mathrm{SB}}(\rho) := S_{\mathrm{obs}}^{\mathcal{C}_{\rho,H_B}}(\rho) = -\sum_{ij} p_{ij} \ln \frac{p_{ij}}{d_i \Omega_j^B}.$$

Introducing the marginal probabilities

$$p_i^S := \sum_j p_{ij}, \quad p_j^B := \sum_i p_{ij} \tag{A7}$$

and the classical mutual information

$$I_{\mathrm{cl}}^{\mathcal{C}_{\rho,H_B}}(\rho) := \sum_{ij} p_{ij} \ln \frac{p_{ij}}{p_i^S p_j^B}, \tag{A8}$$

the system-bath observational entropy can be decomposed as

$$S_{\mathrm{SB}}(\rho) = S_{\mathrm{vN}}(\rho_S) + S_{\mathrm{obs}}^{\mathcal{C}_{H_B}}(\rho_B) - I_{\mathrm{cl}}^{\mathcal{C}_{\rho,H_B}}(\rho), \tag{A9}$$

where

$$\rho_B := \mathrm{tr}_S[\rho], \tag{A10}$$

and

$$S_{\mathrm{obs}}^{\mathcal{C}_{H_B}}(\rho_B) := -\sum_j p_j^B \ln \frac{p_j^B}{\Omega_j^B}. \tag{A11}$$

We now relate this entropy to the conventional entropy production of an open quantum system. We assume the initial product state

$$\rho(0) = \rho_S(0) \otimes \pi_B, \quad \pi_B = \frac{e^{-\beta \widetilde{H}_B}}{\widetilde{Z}_B}, \tag{A12}$$

where

$$\widetilde{H}_B := \sum_j E_j \Pi_j^B,$$

$$E_j := -\beta^{-1} \ln \mathrm{tr}_B\big[\Pi_j^B e^{-\beta H_B}\big] + \beta^{-1} \ln \Omega_j^B, \tag{A13}$$

The initial state in Eq. (A12) describes the standard situation in which the small system is prepared independently of a thermal bath. It naturally arises when the system-bath interaction is initially absent or sufficiently weak that initial correlations can be neglected. Thus, π_B is uniform within each bath-energy window. We define the heat absorbed by the bath by

$$Q_\tau := \mathrm{tr}_B[\widetilde{H}_B\{\rho_B(\tau) - \pi_B\}], \quad \rho_B(\tau) := \mathrm{tr}_S[\rho(\tau)]. \tag{A14}$$

The conventional open-system entropy production is

$$\Sigma_\tau := D(\rho(\tau) \,\|\, \rho_S(\tau) \otimes \pi_B). \tag{A15}$$

Using $\ln \pi_B = -\beta \tilde{H}_B - \ln \tilde{Z}_B$, the initial product state $\rho(0) = \rho_S(0) \otimes \pi_B$, and the unitary invariance of the von Neumann entropy, we obtain

$$\begin{aligned} &D(\rho(\tau)\|\rho_S(\tau) \otimes \pi_B) \\ &\quad = -S_{\mathrm{vN}}(\rho(\tau)) + S_{\mathrm{vN}}(\rho_S(\tau)) - \mathrm{tr}[\rho_B(\tau) \ln \pi_B] \\ &\quad = S_{\mathrm{vN}}(\rho_S(\tau)) - S_{\mathrm{vN}}(\rho_S(0)) + \beta \mathrm{tr}[\tilde{H}_B\{\rho_B(\tau) - \pi_B\}] \\ &\quad = \Delta S_{\mathrm{vN}}(\rho_S) + \beta Q_\tau. \end{aligned} \tag{A16}$$

The change in the system-bath observational entropy is denoted by

$$\Delta S_{\mathrm{SB}}(\tau) := S_{\mathrm{obs}}^{\mathcal{C}_{\rho(\tau),H_B}}(\rho(\tau)) - S_{\mathrm{obs}}^{\mathcal{C}_{\rho(0),H_B}}(\rho(0)). \tag{A17}$$

Since the initial state is a product state, its classical mutual information vanishes. Equation (A9) therefore gives

$$\begin{aligned} &\Delta S_{\mathrm{SB}}(\tau) + I_{\mathrm{cl}}^{\mathcal{C}_{\rho(\tau),H_B}}(\rho(\tau)) \\ &\quad = S_{\mathrm{vN}}(\rho_S(\tau)) - S_{\mathrm{vN}}(\rho_S(0)) + S_{\mathrm{obs}}^{\mathcal{C}_{H_B}}(\rho_B(\tau)) - S_{\mathrm{obs}}^{\mathcal{C}_{H_B}}(\pi_B). \end{aligned} \tag{A18}$$

Consequently,

$$\begin{aligned} &\Sigma_\tau - \Delta S_{\mathrm{SB}}(\tau) - I_{\mathrm{cl}}^{\mathcal{C}_{\rho(\tau),H_B}}(\rho(\tau)) \\ &\quad = \beta Q_\tau - S_{\mathrm{obs}}^{\mathcal{C}_{H_B}}(\rho_B(\tau)) + S_{\mathrm{obs}}^{\mathcal{C}_{H_B}}(\pi_B). \end{aligned} \tag{A19}$$

Define the final and initial bath-energy distributions by

$$\alpha_j := \mathrm{tr}_B\big[\Pi_j^B \rho_B(\tau)\big], \tag{A20}$$

$$\pi_j := \mathrm{tr}_B\big[\Pi_j^B \pi_B\big] = \frac{\Omega_j^B e^{-\beta E_j}}{\widetilde{Z}_B}. \tag{A21}$$

Using

$$\ln \frac{\pi_j}{\Omega_j^B} = -\beta E_j - \ln \widetilde{Z}_B, \tag{A22}$$

the right-hand side of Eq. (A19) becomes

$$\beta Q_\tau - S_{\mathrm{obs}}^{\mathcal{C}_{H_B}}(\rho_B(\tau)) + S_{\mathrm{obs}}^{\mathcal{C}_{H_B}}(\pi_B) = \sum_j \alpha_j \ln \frac{\alpha_j}{\pi_j} = D(\alpha\|\pi). \tag{A23}$$

We therefore obtain the exact identity

$$\Sigma_\tau = \Delta S_{\mathrm{SB}}(\tau) + I_{\mathrm{cl}}^{\mathcal{C}_{\rho(\tau),H_B}}(\rho(\tau)) + D(\alpha\|\pi). \tag{A24}$$

Since both the classical mutual information and the relative entropy are non-negative, this identity immediately yields

$$\Sigma_\tau \geqslant \Delta S_{\mathrm{SB}}(\tau) + I_{\mathrm{cl}}^{\mathcal{C}_{\rho(\tau),H_B}}(\rho(\tau)) \geqslant \Delta S_{\mathrm{SB}}(\tau). \tag{A25}$$

Thus, the system-bath observational entropy provides a coarse-grained description of the conventional entropy production. If the final bath-energy distribution remains close to its initial equilibrium distribution, then $D(\alpha\|\pi)$ is small and Eq. (A24) gives

$$\Sigma_\tau \simeq \Delta S_{\mathrm{SB}}(\tau) + I_{\mathrm{cl}}^{\mathcal{C}_{\rho(\tau),H_B}}(\rho(\tau)). \tag{A26}$$

2. Local-energy coarse graining

The Hamiltonian is decomposed as

$$H = \sum_{\ell=1}^m H_\ell + H_{\mathrm{int}}, \tag{A27}$$

where H_ℓ is the local Hamiltonian of region ℓ and H_{int} describes interactions between different regions. Let

$$H_\ell = \sum_{E_\ell} E_\ell \hat{P}_{E_\ell}^{(\ell)} \tag{A28}$$

be the spectral decomposition of H_ℓ. The projectors resolving the local-energy profile are

$$\hat{P}_{\vec{E}} := \bigotimes_{\ell=1}^m \hat{P}_{E_\ell}^{(\ell)}, \quad \vec{E} := (E_1, \ldots, E_m). \tag{A29}$$

The corresponding coarse graining is

$$\mathcal{C}_{\mathrm{loc}H} := \{\hat{P}_{\vec{E}}\}_{\vec{E}}. \tag{A30}$$

The factorized observational entropy is defined by

$$S_{\mathrm{FOE}}(\rho) := S_{\mathrm{obs}}^{\mathcal{C}_{\mathrm{loc}H}}(\rho) = -\sum_{\vec{E}} p_{\vec{E}} \ln \frac{p_{\vec{E}}}{V_{\vec{E}}}, \tag{A31}$$

where

$$p_{\vec{E}} := \mathrm{tr}[\hat{P}_{\vec{E}}\rho], \tag{A32}$$

$$V_{\vec{E}} := \mathrm{tr}[\hat{P}_{\vec{E}}] = \prod_{\ell=1}^m \mathrm{tr}\big[\hat{P}_{E_\ell}^{(\ell)}\big]. \tag{A33}$$

If the state is supported within a single local-energy macrospace $\vec{E}$, then

$$S_{\mathrm{FOE}}(\rho) = \ln V_{\vec{E}} = \sum_{\ell=1}^m \ln \mathrm{tr}\big[\hat{P}_{E_\ell}^{(\ell)}\big]. \tag{A34}$$

Thus, S_{FOE} reduces to the sum of the microcanonical entropies of the individual regions. More generally, it quantifies the entropy associated with a spatially inhomogeneous energy profile.

An initial macrostate with respect to $\mathcal{C}_{\mathrm{loc}H}$ has the form

$$\rho(0) = \bigotimes_{\ell=1}^m \rho_\ell, \quad \rho_\ell = \sum_{E_\ell} p_{\ell,E_\ell} \frac{\hat{P}_{E_\ell}^{(\ell)}}{\mathrm{tr}\big[\hat{P}_{E_\ell}^{(\ell)}\big]}. \tag{A35}$$

For nondegenerate local Hamiltonians, this condition reduces to

$$[\rho_\ell, H_\ell] = 0. \tag{A36}$$

Such states naturally describe local equilibrium: Each spatial region has relaxed with respect to its own local Hamiltonian, while the system as a whole remains out of equilibrium. This description is appropriate when

$$\tau_{\mathrm{local}} \ll \tau_{\mathrm{transport}}, \tag{A37}$$

so that local equilibration occurs much faster than transport between different regions. It therefore provides the natural coarse-grained description of hydrodynamic relaxation and of systems prepared by joining subsystems initially held at different temperatures.

3. Global-energy coarse graining and diagonal entropy

Finally, consider the spectral decomposition of the global Hamiltonian,

$$H(\lambda) = \sum_i E_i(\lambda) \hat{P}_i^{(E)}(\lambda). \tag{A38}$$

The global-energy coarse graining is

$$\mathcal{C}_{H(\lambda)} := \big\{\hat{P}_i^{(E)}(\lambda)\big\}_i. \tag{A39}$$

The corresponding observational entropy is

$$S_D(\rho; H(\lambda)) := S_{\mathrm{obs}}^{\mathcal{C}_{H(\lambda)}}(\rho) = -\sum_i p_i \ln \frac{p_i}{V_i(\lambda)}, \tag{A40}$$

where

$$p_i := \mathrm{tr}\big[\hat{P}_i^{(E)}(\lambda)\rho\big], \tag{A41}$$

$$V_i(\lambda) := \mathrm{tr}\big[\hat{P}_i^{(E)}(\lambda)\big]. \tag{A42}$$

For a nondegenerate Hamiltonian, $V_i(\lambda) = 1$, and this expression reduces to the conventional diagonal entropy

$$S_d(\rho) = -\sum_i \rho_{ii} \ln \rho_{ii}. \tag{A43}$$

The global-energy coarse graining is natural for driven isolated systems, because it retains only the occupation probabilities of the instantaneous energy eigenspaces. Energy-diagonal states include equilibrium Gibbs and microcanonical states. They also arise as diagonal ensembles describing long-time averages after quantum quenches. The diagonal entropy therefore provides a coarse-grained entropy suitable for both equilibrium states and effective stationary states generated by isolated unitary dynamics.

APPENDIX B: A UNITARY TRANSFORMATION THAT PRESERVES THE GIBBS ENTROPY

For any passive state ρ, we show that the unitary operator that preserves the Gibbs entropy is unique up to phases and is given by

$$U_{\mathrm{ad}} := \sum_i |i_\tau\rangle\langle i_0|. \tag{B1}$$

Here, $\{|i_0\rangle\}_{i=1}^D$ and $\{|i_\tau\rangle\}_{i=1}^D$ are the eigenstates of the initial Hamiltonian $H(\lambda_0)$ and the final Hamiltonian $H(\lambda_\tau)$, respectively, ordered by increasing eigenvalues.

Let U be a unitary operator that preserves the Gibbs entropy. Then, for any passive state ρ,

$$\sum_{i=1}^d \langle i_\tau|U\rho U^\dagger|i_\tau\rangle \ln i = \sum_{i=1}^d \langle i_0|\rho|i_0\rangle \ln i. \tag{B2}$$

It follows that, for the extended microcanonical state, $\rho_{\mathrm{em}}(\Omega) := \frac{1}{\Omega}\sum_{i=1}^{\Omega} |i_0\rangle\langle i_0|$ $(1 \leqslant \Omega \leqslant d)$,

$$\sum_{i=1}^d \sum_{j=1}^{\Omega} |\langle i_\tau|U|j_0\rangle|^2 \ln i = \sum_{i=1}^{\Omega} \ln i. \tag{B3}$$

Starting with the case $\Omega = 1$, the above equation reduces to

$$\sum_{i=1}^d |\langle i_\tau|U|1_0\rangle|^2 \ln i = 0. \tag{B4}$$

If U satisfied $\langle i_\tau|U|1_0\rangle \neq 0$ for some $i > 1$, then

$$\sum_{i=1}^d |\langle i_\tau|U|1_0\rangle|^2 \ln i > 0 \tag{B5}$$

would hold, which leads to a contradiction. Therefore, $\langle i_\tau|U|1_0\rangle = 0$ for $i > 1$ and $|\langle 1_\tau|U|1_0\rangle| = 1$. By unitarity, $\sum_i |\langle 1_\tau|U|i_0\rangle|^2 = 1$, and hence $|\langle 1_\tau|U|i_0\rangle|^2 = \delta_{1i}$. Next, considering the case $\Omega = 2$, we obtain

$$\sum_{i=2}^d |\langle i_\tau|U|2_0\rangle|^2 \ln i = \ln 2. \tag{B6}$$

By the same reasoning as in the case $\Omega = 1$, we obtain $|\langle i_\tau|U|2_0\rangle| = |\langle 2_\tau|U|i_0\rangle| = \delta_{i2}$. Repeating the same argument sequentially up to $\Omega = d - 1$, we obtain $|\langle i_\tau|U|j_0\rangle| = \delta_{ij}$.

APPENDIX C: THE PROOF OF EQ. (29)

The derivation follows Ref. [18]. At first, we show that $\mathcal{W}_q(\rho,\sigma) \leqslant \frac{1}{2}\sum_i |\lambda_\rho^\downarrow(i) - \lambda_\sigma^\downarrow(i)|$. We consider

$$\rho = \sum_i \lambda_\rho(i)|i_\rho\rangle\langle i_\rho|, \quad \sigma = \sum_i \lambda_\sigma(i)|i_\sigma\rangle\langle i_\sigma|. \tag{C1}$$

Here, $\lambda_X(i)$ denotes the ith nonincreasing eigenvalue of the operator X, and $|i_X\rangle$ is the corresponding eigenvector. We consider $W = \sum_i |i_\sigma\rangle\langle i_\rho|$. By definition, we obtain

$$\begin{aligned}\mathcal{W}_q(\rho,\sigma) &= \frac{1}{2}\min_{VV^\dagger=1} \|V\rho V^\dagger - \sigma\| \leqslant \frac{1}{2}\|W\rho W^\dagger - \sigma\| \\ &= \frac{1}{2}\sum_i |\lambda_\rho^\downarrow(i) - \lambda_\sigma^\downarrow(i)|.\end{aligned} \tag{C2}$$

Next, we show $\mathcal{W}_q(\rho,\sigma) \geqslant \frac{1}{2}\sum_i |\lambda_\rho^\downarrow(i) - \lambda_\sigma^\downarrow(i)|$. For any Hermitian operators A and B, let $\eta_i(A)$ and $\eta_i(B)$ denote their singular values arranged in nondecreasing order. Then,

$$\|A - B\| = \sum_i |\eta_i(A - B)| \geqslant \sum_i |\eta_i(A) - \eta_i(B)| \tag{C3}$$

holds [53]. By setting $A = V\rho V^\dagger, B = \sigma$, we obtain the desired inequality. Therefore, $\mathcal{W}_q(\rho,\sigma) = \frac{1}{2}\sum_i |\lambda_\rho^\downarrow(i) - \lambda_\sigma^\downarrow(i)|$ follows.

APPENDIX D: BOUNDS FOR NONTHERMODYNAMIC ENTROPY PRODUCTION

Here, as an application of the main results in Eqs. (40) and (42) to a nonthermodynamic entropy, we consider the entanglement entropy.

Let $|\Psi\rangle_{AB}$ be a pure state on the bipartite Hilbert space $\mathcal{H}_A \otimes \mathcal{H}_B$. We write its Schmidt decomposition as

$$|\Psi\rangle_{AB} = \sum_\alpha \sum_{a=1}^{d_\alpha} \sqrt{\lambda_\alpha}\,|\alpha, a\rangle_A \otimes |\alpha, a\rangle_B, \quad \sum_\alpha d_\alpha \lambda_\alpha = 1. \tag{D1}$$

Here, λ_α denotes a distinct Schmidt eigenvalue, and d_α is its degeneracy. The reduced density matrix on subsystem A is then given by

$$\rho_A = \mathrm{tr}_B[|\Psi\rangle\langle\Psi|] = \sum_\alpha \lambda_\alpha \hat{P}_\alpha^A, \quad \hat{P}_\alpha^A = \sum_{a=1}^{d_\alpha} |\alpha, a\rangle_A\langle\alpha, a|_A. \tag{D2}$$

We define projectors on the total Hilbert space $\mathcal{H}_A \otimes \mathcal{H}_B$ by

$$\hat{Q}_\alpha^{AB} := \sum_{a=1}^{d_\alpha} (|\alpha, a\rangle_A \otimes |\alpha, a\rangle_B)({}_A\langle\alpha, a| \otimes {}_B\langle\alpha, a|) \tag{D3}$$

and

$$\hat{Q}_0^{AB} := \hat{1}_{AB} - \sum_\alpha \hat{Q}_\alpha^{AB}. \tag{D4}$$

These projectors define a coarse graining of the total Hilbert space. We denote this state-dependent coarse graining by

$$\mathcal{C}_{\mathrm{ent}}(\Psi) := \{\hat{Q}_\alpha^{AB}\}_\alpha \cup \{\hat{Q}_0^{AB}\}. \tag{D5}$$

For the pure state $\rho_{AB} = |\Psi\rangle\langle\Psi|$, the probability and volume associated with $\hat{Q}_\alpha^{AB}$ are, respectively,

$$p_\alpha = \mathrm{tr}\big[\hat{Q}_\alpha^{AB}\rho_{AB}\big] = d_\alpha\lambda_\alpha, \quad V_\alpha = \mathrm{tr}\big[\hat{Q}_\alpha^{AB}\big] = d_\alpha. \tag{D6}$$

Moreover, $p_0 = 0$. Therefore, the observational entropy of the total system with respect to the coarse-graining $\mathcal{C}_{\mathrm{ent}}(\Psi)$ is

$$S_{\mathrm{obs}}^{\mathcal{C}_{\mathrm{ent}}(\Psi)}(\rho_{AB}) = -\sum_\alpha p_\alpha \ln\frac{p_\alpha}{V_\alpha} \tag{D7}$$

$$= -\sum_\alpha d_\alpha\lambda_\alpha \ln\lambda_\alpha \tag{D8}$$

$$= S_{\mathrm{vN}}(\rho_A). \tag{D9}$$

Since ρ_{AB} is pure, $S_{\mathrm{vN}}(\rho_A)$ is the entanglement entropy between A and B. Hence,

$$S_{\mathrm{obs}}^{\mathcal{C}_{\mathrm{ent}}(\Psi)}(|\Psi\rangle\langle\Psi|) = S_{\mathrm{ent}}^{(A:B)}(|\Psi\rangle). \tag{D10}$$

Thus, the entanglement entropy of a bipartite pure state can be regarded as the observational entropy of the total system associated with the Schmidt-correlated coarse-graining $\mathcal{C}_{\mathrm{ent}}(\Psi)$.

Using this observation, the main results in Eqs. (40) and (42) yield bounds on the entanglement entropy production

$$\Delta S_{\mathrm{ent}}^{(A:B)}(\tau) := S_{\mathrm{ent}}^{(A:B)}(|\Psi(\tau)\rangle) - S_{\mathrm{ent}}^{(A:B)}(|\Psi(0)\rangle). \tag{D11}$$

Specifically, assuming that the initial state is a product state,

$$|\Psi(0)\rangle = |\psi\rangle_A \otimes |\psi'\rangle_B, \tag{D12}$$

we obtain

$$\Delta S_{\mathrm{ent}}^{(A:B)}(\tau) = S_{\mathrm{ent}}^{(A:B)}(|\Psi(\tau)\rangle) \geqslant 2\mathcal{W}_q\big(\rho_{\mathcal{C}_{\mathrm{ent}}(\Psi(\tau))}(\tau), |\Psi(0)\rangle\langle\Psi(0)|\big)^2 \tag{D13}$$

and

$$\tau \geqslant \frac{2\mathcal{W}_q\big(\rho_{\mathcal{C}_{\mathrm{ent}}(\Psi(\tau))}(\tau), |\Psi(0)\rangle\langle\Psi(0)|\big)^2}{\bar{\sigma}_{\mathrm{ent}}^{(A:B)}},$$

$$\bar{\sigma}_{\mathrm{ent}}^{(A:B)} := \frac{\Delta S_{\mathrm{ent}}^{(A:B)}(\tau)}{\tau}. \tag{D14}$$

APPENDIX E: THE LENARD-TASAKI INEQUALITY

The derivation follows Ref. [36]. Consider an observable F and a probability distribution u satisfying $i < j \Rightarrow F_i \leqslant F_j$ and $u(i) \geqslant u(j)$. Let T be a doubly stochastic matrix and define $v = Tu$. We show that $\langle F\rangle_v \geqslant \langle F\rangle_u$. Introducing $u_a(i) = \Theta(a-i)/a$, we expand $u = \sum_a c_a u_a$, $c_a := a\{u(a) - u(a+1)\}$, $v_a := Tu_a$. Then, we obtain

$$\begin{aligned}
\langle F\rangle_v - \langle F\rangle_u &= \sum_i F_i(v(i) - u(i)) \\
&= \sum_a c_a \sum_i F_i(v_a(i) - u_a(i)) \\
&= \sum_a c_a \Bigg[\sum_{i\geqslant a+1} F_i(v_a(i) - u_a(i)) \\
&\quad + \sum_{i\leqslant a} F_i(v_a(i) - u_a(i))\Bigg] \\
&\geqslant \sum_a c_a \Bigg[F_{a+1}\sum_{i\geqslant a+1}(v_a(i) - u_a(i)) \\
&\quad + F_a\sum_{i\leqslant a}(v_a(i) - u_a(i))\Bigg] \\
&\geqslant \sum_a c_a F_a \Bigg[\sum_{i\geqslant a+1}(v_a(i) - u_a(i)) \\
&\quad + \sum_{i\leqslant a}(v_a(i) - u_a(i))\Bigg] = 0.
\end{aligned} \tag{E1}$$

The first inequality follows from the doubly stochasticity of the map, which implies $i \geqslant a+1 \Rightarrow v_a(i) - u_a(i) \geqslant 0$, $\quad i \leqslant a \Rightarrow v_a(i) - u_a(i) \leqslant 0$. The transition from $p_0^\downarrow$ to $p_t^\downarrow$ can be realized by a doubly stochastic matrix. Choosing the observable as $F_i = -\ln p_t^\downarrow(i)$, we note that $p_t^\downarrow$ is ordered in descending order, so F_i is nondecreasing in i. Since $p_0^\downarrow$ is also descending, all assumptions of the theorem are satisfied. Therefore,

$$\sum_i -\ln p_t^\downarrow(i)(p_t^\downarrow(i) - p_0^\downarrow(i)) \geqslant 0. \tag{E2}$$

[1] L. Mandelstam and I. Tamm, The uncertainty relation between energy and time in non-relativistic quantum mechanics, in *Selected Papers*, edited by B. M. Bolotovskii, V. Y. Frenkel, and R. Peierls (Springer, Berlin, Heidelberg, 1991), pp. 115–123.

[2] N. Margolus and L. B. Levitin, The maximum speed of dynamical evolution, Physica D **120**, 188 (1998).

[3] P. J. Jones and P. Kok, Geometric derivation of the quantum speed limit, Phys. Rev. A **82**, 022107 (2010).

[4] S. Deffner and S. Campbell, Quantum speed limits: From Heisenberg's uncertainty principle to optimal quantum control, J. Phys. A: Math. Theor. **50**, 453001 (2017).

[5] M.-H. Yung, Quantum speed limit for perfect state transfer in one dimension, Phys. Rev. A **74**, 030303(R) (2006).

[6] T. Caneva, M. Murphy, T. Calarco, R. Fazio, S. Montangero, V. Giovannetti, and G. E. Santoro, Optimal control at the quantum speed limit, Phys. Rev. Lett. **103**, 240501 (2009).

[7] S. Lloyd, Ultimate physical limits to computation, Nature (London) **406**, 1047 (2000).

[8] S. Deffner and E. Lutz, Generalized Clausius inequality for nonequilibrium quantum processes, Phys. Rev. Lett. **105**, 170402 (2010).

[9] N. Shiraishi, K. Funo, and K. Saito, Speed limit for classical stochastic processes, Phys. Rev. Lett. **121**, 070601 (2018).

[10] S. Ito, Stochastic thermodynamic interpretation of information geometry, Phys. Rev. Lett. **121**, 030605 (2018).

[11] S. Ito and A. Dechant, Stochastic time evolution, information geometry, and the Cramér-Rao bound, Phys. Rev. X **10**, 021056 (2020).

[12] V. T. Vo, T. Van Vu, and Y. Hasegawa, Unified approach to classical speed limit and thermodynamic uncertainty relation, Phys. Rev. E **102**, 062132 (2020).

[13] K. Yoshimura and S. Ito, Thermodynamic uncertainty relation and thermodynamic speed limit in deterministic chemical reaction networks, Phys. Rev. Lett. **127**, 160601 (2021).

[14] K. Funo, N. Shiraishi, and K. Saito, Speed limit for open quantum systems, New J. Phys. **21**, 013006 (2019).

[15] E. Aurell, C. Mejía-Monasterio, and P. Muratore-Ginanneschi, Optimal protocols and optimal transport in stochastic thermodynamics, Phys. Rev. Lett. **106**, 250601 (2011).

[16] C. Villani, *Optimal Transport: Old and New*, *Grundlehren der mathematischen Wissenschaften* (Springer, Berlin, 2008), Vol. 338.

[17] J.-D. Benamou and Y. Brenier, A computational fluid mechanics solution to the Monge-Kantorovich mass transfer problem, Numer. Math. **84**, 375 (2000).

[18] T. Van Vu and K. Saito, Thermodynamic unification of optimal transport: Thermodynamic uncertainty relation, minimum dissipation, and thermodynamic speed limits, Phys. Rev. X **13**, 011013 (2023).

[19] H. Tasaki, From quantum dynamics to the canonical distribution: General picture and a rigorous example, Phys. Rev. Lett. **80**, 1373 (1998).

[20] A. J. Short, Equilibration of quantum systems and subsystems, New J. Phys. **13**, 053009 (2011).

[21] S. Trotzky, Y.-A. Chen, A. Flesch, I. P. McCulloch, U. Schollwöck, J. Eisert, and I. Bloch, Probing the relaxation towards equilibrium in an isolated strongly correlated one-dimensional Bose gas, Nat. Phys. **8**, 325 (2012).

[22] M. Cramer and J. Eisert, A quantum central limit theorem for non-equilibrium systems: Exact local relaxation of correlated states, New J. Phys. **12**, 055020 (2010).

[23] N. Shiraishi and H. Tasaki, Nature abhors a vacuum: A simple rigorous example of thermalization in an isolated macroscopic quantum system, J. Stat. Phys. **191**, 82 (2024).

[24] A. M. Kaufman, M. E. Tai, A. Lukin, M. Rispoli, R. Schittko, P. M. Preiss, and M. Greiner, Quantum thermalization through entanglement in an isolated many-body system, Science **353**, 794 (2016),.

[25] H. Tasaki, Quantum statistical mechanical derivation of the second law of thermodynamics: A hybrid setting approach, Phys. Rev. Lett. **116**, 170402 (2016).

[26] A. Hokkyo and M. Ueda, Universal upper bound on ergotropy and no-go theorem by the eigenstate thermalization hypothesis, Phys. Rev. Lett. **134**, 010406 (2025).

[27] F. Meier, T. Rivlin, T. Debarba, J. Xuereb, M. Huber, and M. P. Lock, Emergence of a second law of thermodynamics in isolated quantum systems, PRX Quantum **6**, 010309 (2025).

[28] F. Brandão, M. Horodecki, N. Ng, J. Oppenheim, and S. Wehner, The second laws of quantum thermodynamics, Proc. Natl. Acad. Sci. USA **112**, 3275 (2015).

[29] D. Šafránek, J. M. Deutsch, and A. Aguirre, Quantum coarse-grained entropy and thermalization in closed systems, Phys. Rev. A **99**, 012103 (2019).

[30] P. Strasberg and A. Winter, First and second law of quantum thermodynamics: A consistent derivation based on a microscopic definition of entropy, PRX Quantum **2**, 030202 (2021).

[31] J. Schindler and A. Winter, Continuity bounds on observational entropy and measured relative entropies, J. Math. Phys. **64**, 092201 (2023).

[32] R. Hamazaki, Speed limits for macroscopic transitions, PRX Quantum **3**, 020319 (2022).

[33] T. N. Ikeda, N. Sakumichi, A. Polkovnikov, and M. Ueda, The second law of thermodynamics under unitary evolution and external operations, Ann. Phys. **354**, 338 (2015).

[34] A. Polkovnikov, Microscopic diagonal entropy and its connection to basic thermodynamic relations, Ann. Phys. **326**, 486 (2011).

[35] J. W. Gibbs, *Elementary Principles in Statistical Mechanics: Developed with Special Reference to the Rational Foundation of Thermodynamics* (Charles Scribner's Sons, New York, 1902).

[36] H. Tasaki, Statistical mechanical derivation of the second law of thermodynamics, arXiv:cond-mat/0009206.

[37] J. Dunkel and S. Hilbert, Consistent thermostatistics forbids negative absolute temperatures, Nat. Phys. **10**, 67 (2014).

[38] R. H. Swendsen and J.-S. Wang, Gibbs volume entropy is incorrect, Phys. Rev. E **92**, 020103(R) (2015).

[39] S. Braun, J. P. Ronzheimer, M. Schreiber, S. S. Hodgman, T. Rom, I. Bloch, and U. Schneider, Negative absolute temperature for motional degrees of freedom, Science **339**, 52 (2013).

[40] N. F. Ramsey, Thermodynamics and statistical mechanics at negative absolute temperatures, Phys. Rev. **103**, 20 (1956).

[41] N. Shiraishi and K. Saito, Speed limit for open systems coupled to general environments, Phys. Rev. Res. **3**, 023074 (2021).

[42] G. Lindblad, On the generators of quantum dynamical semigroups, Commun. Math. Phys. **48**, 119 (1976).

[43] V. Gorini, A. Kossakowski, and E. C. G. Sudarshan, Completely positive dynamical semigroups of *N*-level systems, J. Math. Phys. **17**, 821 (1976).

[44] M. Demirplak and S. A. Rice, Adiabatic population transfer with control fields, J. Phys. Chem. A **107**, 9937 (2003).

[45] M. V. Berry, Transitionless quantum driving, J. Phys. A: Math. Theor. **42**, 365303 (2009).

[46] S. Campbell and S. Deffner, Trade-off between speed and cost in shortcuts to adiabaticity, Phys. Rev. Lett. **118**, 100601 (2017).

[47] K. Funo, J.-N. Zhang, C. Chatou, K. Kim, M. Ueda, and A. del Campo, Universal work fluctuations during shortcuts to adiabaticity by counterdiabatic driving, Phys. Rev. Lett. **118**, 100602 (2017).

[48] Z. Sun, L. Zhou, G. Xiao, D. Poletti, and J. Gong, Finite-time Landau-Zener processes and counterdiabatic driving in open systems: Beyond Born, Markov, and rotating-wave approximations, Phys. Rev. A **93**, 012121 (2016).

[49] A. W. Marshall, I. Olkin, and B. C. Arnold, *Inequalities: Theory of Majorization and its Applications*, 2nd ed., Springer Series in Statistics (Springer, New York, NY, 2011).

[50] T. M. Cover and J. A. Thomas, *Elements of Information Theory*, *Wiley Series in Telecommunications and Signal Processing*, 2nd ed. (Wiley-Interscience, Hoboken, NJ, 2006).

[51] M. A. Nielsen and I. L. Chuang, *Quantum Computation and Quantum Information*, 10th ed. (Cambridge University Press, Cambridge, UK, 2010).

[52] K. M. R. Audenaert, A sharp continuity estimate for the von Neumann entropy, J. Phys. A: Math. Theor. **40**, 8127 (2007).

[53] R. Bhatia, *Matrix Analysis* (Springer, New York, 1997).